2011

The transient wave effect and real losses correlation-frequency, temporal, and spatial analysis

Dina Sa Knight
Louisiana State University and Agricultural and Mechanical College

THE TRANSIENT WAVE EFFECT AND REAL LOSSES CORRELATION - FREQUENCY, TEMPORAL, AND SPATIAL ANALYSIS

A Thesis

Submitted to the Graduate Faculty of the
Louisiana State University and
Agricultural and Mechanical College
in partial fulfillment of the
requirements for the degree of
Master of Science

in

The Interdepartmental Program in Engineering Science

by
Dina Sa Knight
B.A., Rutgers, The State University of New Jersey, 1988
December 2011

ACKNOWLEDGMENTS

The author wishes to acknowledge the unending support and constant inspiration of Dr. Clinton Willson, Graduate Coordinator and Associate Professor of Civil and Environmental Engineering. Additional thanks go to Dr. W. David Constant, Dean of The LSU Graduate School and Humphreys T Turner Professor of Civil and Environmental Engineering, and Dr. Kevin S. McCarter, Associate Professor of Experimental Statistics, for graciously agreeing to contribute as a committee and as experts in their respective fields. Dr. Don J. Wood, Professor Emeritus, University of Kentucky, and Director of KYPIPE LLC, for courteously allowing the use of his graphics and for his instruction. Mr. Eugene Owen, Chairman of Utilities Holding, Inc., for his enthusiasm, motivation, invaluable knowledge, and contribution. The author thanks The Baton Rouge Water Works Company for allowing this research to materialize. Specifically, Mr. Patrick Kerr, President and Chief Executive Officer, for his immediate support that is greatly appreciated. Mr. Vincent Dimattia, Engineering Manager, for his willingness to share his forty plus years of knowledge. The author also thanks Mr. Randy Hollis, President of Owen & White, Consulting Engineers, Inc., for his numerous ideas and contributions to this research. Mr. Chris Morris, Hydraulic Systems Analyst at Owen & White, Consulting Engineers, Inc., for his surge analysis and contribution to this research. The author is forever grateful to the late Dr. Roy K. Dokka, Fruehan Endowed Professor of Engineering, for effectively convincing the author to join the Engineering Science program at the School of Engineering. In fact, he insisted. Finally, the author wishes to thank her husband, brother, and mother, for their "you can do it… just go do it" attitude.

TABLE OF CONTENTS

LIST OF TABLES

LIST OF FIGURES

ABSTRACT

Water distribution systems are prone to transients since pumps need to be started and stopped, pumps may have sudden flow changes, human blunders can occur, equipment may fail, or other unavoidable natural events may ensue. Surge modeling techniques are available to calculate variations in pressure, under extreme or normal operating conditions, serving as a tool to predict extreme events in order to design a suitable system and, or, to aid in the implementation of proper measures to mitigate transients. However, modeling an entire water network system may not be cost effective and may require extensive research and time especially in large distribution systems. Spatial analysis may offer an efficient alternative method of uncovering areas with potential problems. In this research, spatial statistic methods were employed to find whether clustering of leak events is occurring, the distance at which the leak clustering is most prevalent, and the location of the leak concentrations. Specifically, the following spatial statistic methods were utilized: nearest neighbor, Ripley's K-function, and the G_i* local statistic. The objective for this research was to locate stations with high concentrations of leaks and whether these leak clusters were related to pump trips due to power failures. Although the concentration of leaks was found near two stations, a correlation between the cluster of leaks and the pump trips was not established.

CHAPTER 1
INTRODUCTION

1.1 Study Area

The Baton Rouge Water Company (BRWC) serves an area of roughly one hundred and fifty square miles and has approximately 8.1 million linear feet of water mains. Over two hundred and forty thousand customers in the region rely on the service provided by the Company. This water system is composed of 65 wells, 39 pump stations, 15 house pumps, 12 enclosed storage facilities, 1 station with solely a booster pump, and 1 reservoir. Founded in 1910, the Company is faced with aging infrastructure and fragile pipe materials, such as asbestos cement, that may be more vulnerable to transient wave conditions that can damage pipes and lead to water losses. The Company's water system is comprised largely of cast iron (roughly 41%), polyvinyl chloride (roughly 23%), and asbestos cement (roughly 18%); the remainder 18% of mains are permastrand, steel, ductile iron, tubing, galvanized, polyethylene, and copper.

1.2 Water Loss

Water loss can be classified as apparent or real. Apparent losses involve such factors as errors in the metering system, unauthorized consumption, unmeasured use, and billing and consumption errors. Real losses involve issues with the physical system such as leaks from pipes, joints, fittings, tanks, hydrants, reservoir, and reservoir overflow.

Real water loss stems from leaks in the water system that may or may not be easily detectable. Many leaks occur below the ground and often seep into the drainage system not surfacing to the ground level where they can be detected. Several factors may cause leaks in the system but one possible cause has recently come into focus by some researchers, the transient wave effect.

1.3 Transient Wave Effect

Water main leaks may occur from pipes damaged by transient wave effect. One of these transient effects arises from rapid fluid velocity changes that can generate extremely low and high pressure spikes in the distribution system. The low pressure point disperses as a low pressure, high velocity wave thus creating water column separation in the pipes. Vacuum pressures develop within the pipe that, depending on the duration, may cause vapor cavities which can have adverse effects on pipes such as pipe collapse. The collapse of the vapor cavities as the pipeline re-pressurizes generates localized low and high pressures that can cause pipe failure (Phalempin, 2009).

Transient wave conditions are normally evaluated to prevent extreme events that occur due to rapid changes such as power failures. However, a transient wave can travel roughly 1 mile in a mere 1.5 seconds at speeds up to 4,000 fps (feet per second) (under normal circumstances water travels in the pipe at about 5-6 fps) depending on pipe characteristics. Generators located at stations with pumps providing back-up power, require about a 35-45 second initiation. The inherent delay in the starting of the generators prevents the units from initiating swiftly enough to keep a pump running. This delay provides plenty of opportunity for the creation of a transient event in the absence of appropriate precautionary measures. If the transient wave encounters a capped end, for example, it will travel back to the source at the same speed and time. If measures are not taken to mitigate the power in the transient wave, damage to piping, valves, or pumps can occur. Thus, fluctuations in the flow state can adversely affect water pipes and assets (Hollis, pers. comm.).

Surge models are available that attempt to predict and simulate the extent of transients and variations in pressure under current or hypothetical conditions of a system. However,

modeling an entire distribution system in a proper manner, accounting for the specific characteristics of the system in question, requires extensive research and time. Spatial analysis may be beneficial to perform in large distribution systems, such as the Baton Rouge Water Company's system, in an effort to isolate areas of concern. Thence, the areas of concern can be further investigated.

The transient wave effect will be explored in this research as a factor in real losses. Specifically, this research will attempt to explain the leaks produced from the damaging effects of power-outage-created transient wave events.

1.3 Objectives

Power failures create transient wave events that lead to pipe damage and leaks (water loss). Therefore, geographical concentration of leaks near a pump station may indicate that pressure fluctuations and power outage events may have a correlation. Spatial analysis methods offer a manageable approach to identifying locations of concentrations on which to focus further examination and to perform time-intensive methods such as surge modeling.

Thus, performing analysis to find the concentration of leaks, the frequency of leaks, power outage time of occurrence, and power outage frequency should detect a relationship, or the lack thereof, with transient wave events.

The main tasks performed are as follows: 1) Data containing the location of main, hydrant, service, and meter leaks over the past thirty nine months (October, 2006 – January, 2010) is geocoded (mapped) in order to examine the spatial distribution and the temporal distribution of the leaks. The proposed method of analysis is the application of spatial statistics; specifically, average nearest neighbor, multi-distance spatial autocorrelation (Ripley's K function), and hot-spot analysis (Gi* statistic). 2) Data containing station outages is examined to

review the temporal dispersion and the frequency of station power outages over the past thirty nine months. 3) Then, a comparison is performed between the concentration and frequency of leaks with the frequency, location, and time of power outages. 4) The stations that exhibit statistically significant leak concentrations are compared to transient (surge) wave models generated of the stations isolated by the spatial analysis.

CHAPTER 2
LITERATURE REVIEW

2.1 Water Loss

Water supply seemed plentiful and infinite for many years in most of the world's water systems. Therefore, water loss was largely disregarded and considered an intrinsic part of a water supplying operation. However, the growth of our cities, the limits of water resources, and regulation costs have forced the industry to evaluate its operations. Surprisingly, water loss control is not widely practiced worldwide (Thornton, Sturm, Kunkel, 2008).

There are two principally recognized types of water loss: Real and apparent losses. Apparent losses are not produced by the physical loss of water but are rather due to errors in consumption and billing as well as metering errors and unmeasured or illegal consumption. However, apparent losses can have a large impact on revenues and is an important aspect of water loss (Thornton, Sturm, Kunkel, 2008).

Real losses occur in the physical distribution system in which the water seeps from pipes, fittings, joints, hydrants, enclosed storage facilities (e.g. tanks), and reservoirs. It is also an important aspect of water loss. This research project will deal only with the real loss category (Thornton, Sturm, Kunkel, 2008).

Real losses are typically either reported, unreported, or background leaks. Reported leaks are usually breaks that cause high flow rates, are easily detectable, cause service disruptions, and are, therefore, reported within a short period of time. Conversely, unreported leaks have medium flow rates, are not easily detectable, run for long periods of time, and are usually found by leak detection equipment. Background leaks are seepages in pipe joints and connections too small to even be exposed by leak detection equipment. They run for quite long periods of time slowly worsening until reaching the point of being detectable. Background leakage reduction is possible

through pressure management and replacement of faulty infrastructure (Thornton, Sturm, Kunkel, 2008).

Reported events that involve large main breaks are perceived to have the largest impact in water loss. However, these events are usually short in duration since these disruptions in service are quickly resolved. Small concealed leaks, on the contrary, can cause much larger volumes of water loss and can potentially run for years before they are detected and repaired. Recently, the relationships between pressure and leakage rates demonstrate that certain leaks, such as joint leaks (usually found in AC piping or old hydraulic couplings), are extremely vulnerable to fluctuations in pressure; PVC or plastic based pipes and high background leakages are also vulnerable to pressure fluctuations (Thornton, Sturm, Kunkel, 2008).

Remote sensor technologies, such as the Supervisory Control and Data Acquisition (SCADA) system, monitor the water distribution system and can aid in the isolation of leaks on a large scale. The data provided by the SCADA system can be used for analysis of source (pump stations and tanks), transmission lines, and of the distribution system (Beecher, Flowers, 1999).

2.2 Surge Pressure

There are two types of pressure surges: transient and cyclic. Cyclic pressure surging, as the name implies, is recurring in nature by the fluctuating action of equipment such as reciprocating pumps, un-dampened pressure control valves or interacting pressure regulating valves, wavering demand, etc. Cyclic surges may result in fatigue damage. Transient surges occur in a rapid period of time shifting from one steady state to another. This is commonly termed as water hammer (Moser, Folkman, 2008).

Water main leaks may occur from pipes damaged by transient wave effect. One of these transient effects arises from rapid fluid velocity changes that can generate extremely low and

high pressure spikes in the distribution system. The low pressure point disperses as a low pressure, high velocity wave thus creating water column separation in the pipes (Figure 1). Vacuum pressures develop within the pipe that, depending on the duration, may cause vapor cavities which can have adverse effects on pipes such as pipe collapse. The collapse of vapor cavities as the pipeline re-pressurizes generates localized low and high pressures; high pressures can damage pumps, valves, and cause pipe rupture (Phalempin, 2009).

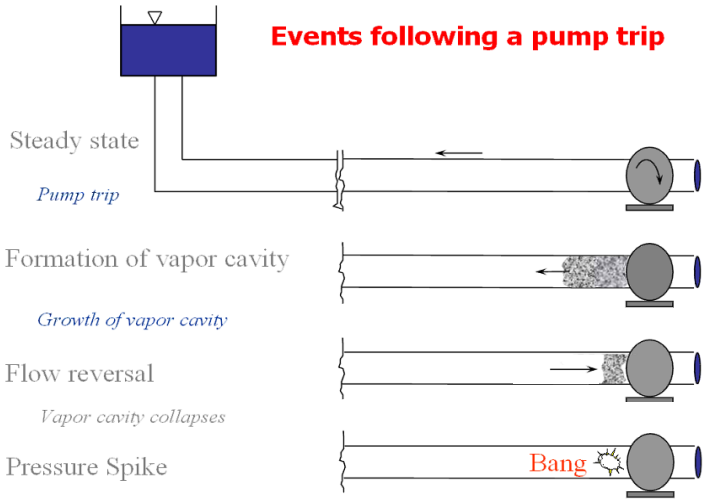

Figure 1. Formation of vapor cavity and its collapse (by permission: Wood, per. comm.)

The degree of severity of transient event pressures, created by a particular change in velocity, is dependent on the geometry of the water system, the amount in velocity change, and the speed of the wave in a particular system. The wave speed is dependent on pipe modulus of elasticity, pipe diameter (the smaller the diameter, the faster the wave speed), pipe thickness (the thinner the walls, the lower the wave speed), fluid modulus of elasticity (the higher the value, the faster the wave speed), pipe restraints (unrestrained pipes allow more movement of the pipe which slows the wave speed), fluid density and modulus (wave speed increases with modulus and decreases

with density of the fluid), and amount of air in the fluid (Moser, Folkman, 2008; Wood, pers. comm.; Hollis, pers. comm.).

Rapid flow changes due to sudden valve closure and pump stoppages may result in large scale pressure waves. Essentially, transient events are disruptions during transitions from one constant state to another. The disrupted state of the pressure waves propagate through the distribution system with sound wave velocity, acoustic or sonic, depending on the water properties and pipe elasticity. As the waves spread through the system, transient flow conditions are generated which can lead to equipment damage, system fatigue, and pipe failure. Friction and damping in the system will slowly re-stabilize the waves to a steady state. However, smooth transitions to this state can only be achieved with careful slow flow regulation and in the absence of large fluctuations in pressure and flow. Typically, events that can initiate a sequence of transient waves, which are transmitted and reflected at discontinuities in the system (pipe junctions, pumps, open or closed ends, etc.) fall in the following categories: 1) pump starting and stopping; 2) valve closing and opening; 3) boundary pressure changes such as tank and reservoir water level drop, tank pressure change, etc.; 4) drastic shift in water demand such as in flushing of hydrants; 5) water transmission changes such as main breaks; 6) pipe air releasing; 7) regulator or check valve activity (Wood, 2005).

Transients are likely to occur in water distribution systems since water system pumping units need to be started and stopped, have sudden flow changes, human error, equipment failure, and other natural occurrences that are unavoidable. Transient regimes are most notable at pump stations, control valves, low static pressure spots, high elevation areas, and remote locations distant from tanks. Transients are particularly intense from rapid transitions such as those formed from power failure or emergency valve operations (Jung, Karney, Boulos, Wood, 2007).

Vapor cavity formation is associated with a net flow away from the cavitation point. As such, a pump component in the water system is considered only if and when a vapor pocket formation occurs on the discharge side. An uncontrolled pump shutdown (e.g. 2 second pump run down) can create a severe transient where cavitation occurs (at -14 psig – pounds per square inch gage) and then peaks (e.g. to 150 psig). Sub-atmospheric pressures are likely to occur throughout the water distribution system during this event (Wood, Lingireddy, Boulos, 2005).

Localized drops in pressure can release dissolved gas (air) from the water stimulating corrosion of steel and iron pipes. Consequently, this leads to the formation of rust and pipeline damage. Transient protection such as relief valves or air chambers when improperly designed and regulated, may provide a means for contaminants to enter the water system. In certain circumstances, such as when a main breaks, the normal chlorine residual may not adequately treat the contamination (Wood, Lingireddy, Boulos, 2005).

Transient analysis is a fundamental part of good water distribution system design and operation and is an integral part in estimating worst-case scenarios. However, the transient effect in distribution systems are susceptible to unique characteristics and simplified analysis methods may result in deficient surge protection. Furthermore, the implications of water quality from leaks due to pressure fluctuation disturbances can result in the detachment of biofilm, re-suspension of settled particles, and the intrusion of contaminated groundwater (Jung, Karney, Boulos, Wood, 2007; Wood, Lingireddy, Boulos, Karney, McPherson, 2005).

Transient wave surge design guidelines such as guidelines published by the American Water Works Association (Manual M11, *Steel Water Pipe – A Guide for Design and Installation,* 2004; Manual M23, *PVC [polyvinyl chloride] Pipe – Design and Installation,* 2002*;* and C403-00, *Selection of Asbestos – Cement Transmission Pipe, Sizes 18in. Through 42 in.,* 2000) are

geared largely towards simple systems; a sudden event on a single main pipe. Thus, the seemingly conservative guidelines may actually be insufficient and consequently costly. According to the guidelines, the relationship between pressure increase and the increase in fluid velocity is unrelated to the length of the pipe. However, this does not account for friction losses that can greatly increase or decrease surge pressure nor does it account for the system depth variations. Additionally, pipe diameter, pipe thickness, pipe material type, water elasticity, water density, water temperature, as well as air and solid contents in the water, all affect wave velocity. Some of these characteristics are quite complex and are challenging to ascertain. Although estimates of the highest wave velocity relate to the largest potential wave, it may not necessarily correspond to the actual largest wave surge. The aforementioned characteristics are vital to wave surge analysis and to good dependable design (Jung, Karney, Boulos, Wood, 2007).

Furthermore, general design guidelines pertain to simple, homogeneous water systems whose relationships do not account for dissimilar pipe properties that create distinctive transient surge wave reflections. Nor do they account for the effect of friction. The product of a reflected wave in a single pipe will depend on the characteristics of the pipe at each segment. Thus, the result of this event affects the severity of the transient wave effect (Jung, Karney, Boulos, Wood, 2007).

In a complex system of mains the pipes can be the source of transient waves or act as a transmitter/receiver, and thus, by the nature of its own topology, affecting increases in pressure. Again, the varied pipe functions are important considerations in analysis and design. However, there is a risk of either insufficient or over-sufficient pipe design in that one creates a safety issue and the other a cost issue (Jung, Karney, Boulos, Wood, 2007).

To complicate matters, main networks consist of junctions and dead ends that create wave refractions and reflections with the ability to intensify or diminish wave surges. Distribution systems may lack the adequate surge analysis and design that take into account the varied loadings while focusing on worse-case scenarios (Jung, Karney, Boulos, Wood, 2007).

In terms of maximum pressure, the relatively small rotational inertia produced by contemporary pumps during power outages creates sudden changes that are not particularly rare in occurrence. Consequently, the estimated potential surge, using conventional generalized analysis methods, may not anticipate the ultimate pressures created by a distribution system's diverse dynamics. In the case of loops, designed to provide system reliability and flexibility in complex systems, conventional analysis may draw erroneous assumptions in reference to transient wave effect (Jung, Karney, Boulos, Wood, 2007).

Another shortcoming of some conventional analysis' expressions is that they do not consider liquid column separation. As stated in more detail earlier, pressures below liquid vapor pressure create flow vapor cavities. The collapse of these cavities produces a substantial pressure increase that can damage pipeline systems (Jung, Karney, Boulos, Wood, 2007).

Surge simulation models are available that are capable of accurately predicting transients and pressure fluctuations of a water distribution system. Currently, the two most commonly used approaches in modeling applications are the method of characteristics (MOC) and the wave characteristic method (WCM). The MOC is an accurate technique for surge simulation. However, the MOC requires copious steps or computations to solve common transient issues. In fact, more complex and substantial distribution systems require a greater number of calculations. Conversely, the WCM approach requires fewer flow and pressure calculations and can accommodate large distribution system computations in an effective and efficient manner. The

wave characteristics method is founded on the notion that transient pipe flow is the resulting effect of a disturbance in the system leading to the creation and transmission of pressure waves. .

Although, both the MOC and WCM methods entail numerous calculations to arrive at a solution, the WCM method requires fewer calculations. Both the MOC and the WCM approaches will nearly always arrive at same solution for computations of the same system, with the same data, same model characteristics, and to the same accuracy. Therefore, both approaches can accurately predict transient pressures and flows in a water distribution system (Wood, Lingireddy, Boulos, Karney, McPherson, 2005).

Surge modeling is a suitable tool in designing pre-emptive measures to properly control and prevent fluctuating pressures and disastrous transient events. In any case, surge simulation models require proper development and calibration to effectively predict improper or extreme conditions in a distribution network (Wood, Lingireddy, Boulos, Karney, McPherson, 2005).

Nevertheless, conducting a surge analysis for an entire water system may not be suitable if there is only a mere suspicion of a transient related problem. Additionally, because surge modeling requires meticulous and extensive research an time, an analysis of an entire network, especially a large water system, may not be cost effective. Spatial analysis methods are available to efficiently identify a problem area(s) so as to merit further examination.

2.3 Pipe Characteristics and the Consequences

Pipes of differing materials have characteristics that may make them more or less vulnerable to certain conditions such as surge pressures, vacuum pressures, ground movement (expansive soils), soil subsidence, corrosion, etc.

Expansive soils, primarily expansive clays, are subject to seasonal moisture content fluctuations. In dry periods the soil shrinks. The rewetting over the years causes the soil to swell

imposing lateral and vertical bending on pipes that may lead to longitudinal or circumferential fractures (Holtz, Kovacs, 1981; Owen, pers. comm.).

Corrosion is an electrochemical reaction between a metal and its surroundings. This reaction alters the properties of the metal. Corrosion occurs when the metals in the pipe are not in concert with the water it contacts. Factors that are likely to influence corrosion are: soil resistivity, moisture content, ground water influence, pH of the water, chlorides in the soil, soil sulfides, redox potential (electrical potential of a metal), bi-metallic considerations (pipe connections, stops), and known corrosive environments (HDR Eng. Inc., 2001; DIPRA, 2006).

Cast iron has an elastic modulus value, the tendency to be deformed elastically, between 10×10^6 to 15×10^6 lbs/in^2 (Table 1) depending on the ratio of the pipe's inside diameter to the pipe's wall thickness. Ductile iron is a material that has an elastic modulus value of 24×10^6 lb/in^2. Steel, having the next highest modulus value of 29.5×10^6 lb/in^2, also has the potential for the highest wave speeds (3000-5000 ft/s). In general, rigid pipes such as ductile and cast iron generate high wave speeds (approximately 2000-4500 ft/s) (Figure 2) and are vulnerable to breaks from high pressure spikes. Ductile iron pipe is essentially more flexible or more yielding than gray cast iron. However, it contains similar brittle properties as gray cast iron. The rate of corrosion in ductile iron is also similar to that of gray cast iron. Nevertheless, ductile iron's wall is thinner, therefore, corrosion is more significant. Ductile iron that is lined with cement-mortar contains some corrosion protection and an improved hydraulic efficacy. Ductile iron can withstand a great amount of bending before failing allowing for stress redistribution and for potential stress reduction. Higher strength steel pipes are more brittle and thin steel can collapse under vacuum pressures. Steel is also susceptible to corrosion (Moser, Folkman, 2008; Owen, pers. comm.; Hollis, pers. comm.).

Asbestos cement (AC) is generally considered a rigid pipe. Nevertheless, it does possess some flexibility. The elastic modulus value of AC is 3.4×10^6 lbs/in^2 and is a durable material that is less prone to impact damage as some rigid pipes. Unfortunately, AC pipe is vulnerable to vacuum pressures, breaks from high pressure pipes, and breaks from soil shrink and swell (Moser, Folkman, 2008; Hollis, pers. comm.).

Table 1. Elastic Modulus values

Material	Elastic Modulus
Steel	29.5×10^6 lb/in^2
Ductile Iron	24×10^6 lb/in^2
Cast Iron	10×10^6 to 15×10^6 lbs/in^2
Asbestos Cement	3.4×10^6 lbs/in^2
PVC	4×10^5 lb/in^2
PE	1×10^5 lb/in^2

Thermoplastics include such materials as polyvinyl chloride (PVC), polyethylene (PE), polybutyline (PB), and acrylonitrile-butadiene-styrene (ABS). Thermoplastic pipes such as PVC and PE generate lower wave speeds (generally 1200-1500 ft/s), are corrosion resistant, and have outstanding deformation to earth-load transfer ratio performance characteristics (the ability to undergo localized strains without failure). Sustained operating pressures in the system do not usually lead to failure in PVC piping. However, continuous high cyclic loading along with extreme peak pressures, can result in PVC premature failure. Polyvinyl chloride pipes are not subject to biological deterioration. Conversely, polyethylene pipes are more vulnerable to environmental stress cracking where there is accelerated degradation when contact with particular chemicals and high stress levels act concurrently; there are grades of PE that are highly resistant to stress cracking as well as weather-resistant, and are high in density such as grade P34

(Type III, class C, category 5). Due to polyethylene's rather low elastic modulus value of 100,000 lb/in^2 (or 1 x 10^5 lb/in^2), it is prone to ring compression stresses resulting in circumferential ring shortening. Higher-density PE is characterized by superior stiffness, tensile strength, and hardness along with a decrease in toughness, impact strength (at lower temperatures), and long-term crack resistance. Both PVC and PE are susceptible to collapse under vacuum pressures (Moser, Folkman, 2008; Hollis, pers. comm.).

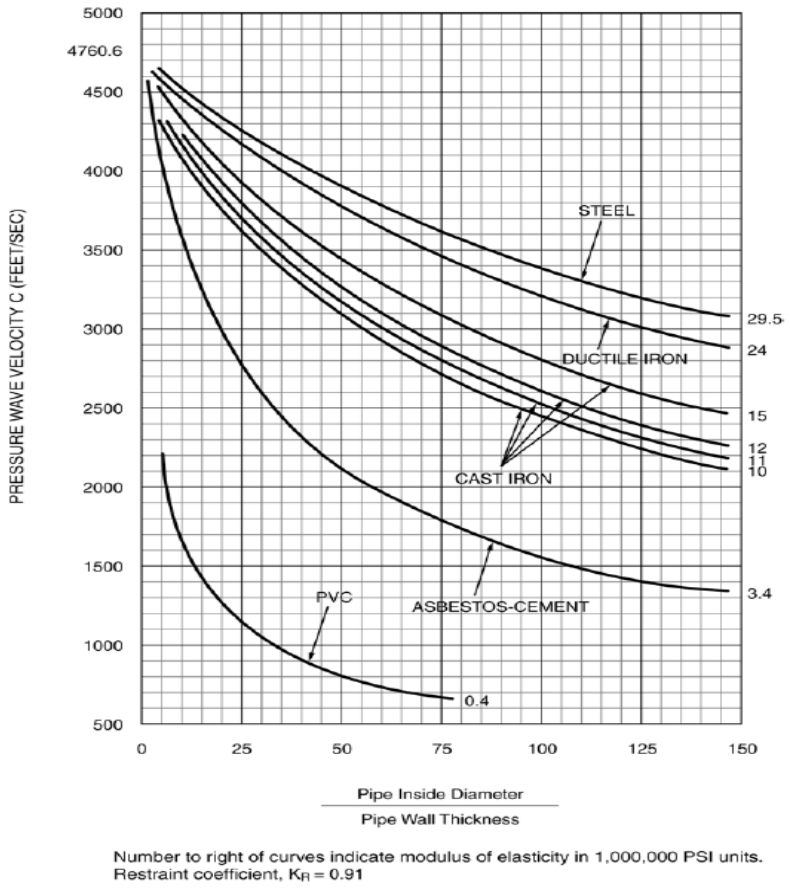

Figure 2. Pressure wave velocity by material (by permission: Wood, pers. comm.)

2.4 Controlling Excessive Pressure Surges

A variety of means exist to provide surge control in the event of a transient wave incident. These measures attempt to alter the flow velocity by dawdling or accelerating in an

adequately gradual manner. Ideally, a mixture of devices may be used to prevent and control upsurges (high pressure events) and downsurges (low pressure events such as a pump power failure). However, because of the complexity of transient behavior, devices meant to control transient conditions, if not properly selected, located, or used, may induce an event (Wood, Lingireddy, Boulos, 2005).

Common surge protection devices include: surge tanks (open, closed, one way, etc.), pressure relief valves, surge anticipation valves, air release/vacuum valves, check valves, pump bypass line, resistive component bypass line (Wood, Lingireddy, Boulos, 2005).

Generally, surge tanks serve the following purposes: 1) prevent high pressures by temporarily storing excess liquid after a shutoffs, 2) prevent low pressure and potential cavitation by temporarily introducing liquid into a region of low pressure in the water system (Wood, Lingireddy, Boulos, 2005).

The purpose of an air release or vacuum valve is to prevent low pressure (cavitation) by drawing air into the pipe when pressure goes below atmospheric in high point areas. Once the pipe pressurizes to above atmospheric, the air is ejected. Nonetheless, air that is ejected too quickly can result in air slams which may create a secondary surge in pressure. Therefore, careful valve selection, use, and location are vital (Wood, Lingireddy, Boulos, 2005).

Pump bypass lines are installed with a check valve to prevent back flow from the pump discharge to the suction side. The bypass prevents the buildup of high pressures on the pump suction side and cavitation on the discharge side. A pump bypass set-up is designed for locations in the system that contains such equipment as a booster pump; where substantial suction head exists. The check valves are one-way flow schemes which prevent flow reversal. However, response time delays and possible rapid opening and closing cycles can cause severe transient

events; significant backflow may occur since these valves do not close instantaneously possibly causing surges. Again, careful design and use of these valves are crucial (Wood, Lingireddy, Boulos, 2005).

2.5 Overview of Spatial Statistical Methods

Spatial statistics allows for the comparison of the spatial distribution of features in a geographic area to an assumed random spatial distribution in order to execute actual spatial pattern analysis. Generally speaking, the basis of comparison is expressed by the dispersion of the values around the mean (standard deviation or variance). A statistical analysis performed in a dataset will show whether a trend or a pattern exists and whether it is statistically significant, that is, if the distribution differs from a random distribution. Geographic spatial statistics analyzes features that are associated with locations on the surface of the earth. The nature of geographic data, data collection and storage methods, and study-area boundary choices affect the outcome of the analysis. Assumptions that patterns and relationships are not influenced by external factors, or observations not influencing one another, or that each observation is equally likely to occur, contradict the nature of geographic data. The equal likelihood that features or values occur at any location does not express the regional and local tendencies of the majority of geographic data (Mitchell, 2009).

In order to identify patterns, a distribution of observed features is compared to a hypothetical random distribution using the same number of features over the same area as the observed number of features and area. A statistic is calculated for the observed and the random distribution. The randomization sampling routine postulates that an observed spatial pattern of the data denotes one of other possible spatial arrangements. The null hypothesis would be that if the random sampling is performed an infinite number of times, the result of the pattern is not

significantly different from the observed pattern. If the null hypothesis is rejected at the specified significance level, the observed pattern of values significantly differs from the random pattern. The degree which the observed distribution departs from the random is the extent that the pattern is either more clustered or more dispersed than the random distribution (Mitchell, 2009).

Spatial statistical methods calculate a test statistic as it calculates the initial statistic. The Z-score is a common measure of test statistic reported in spatial analysis. It is a reference measure for the standard normal with a standard deviation of one and a mean of zero (Mitchell, 2009).

The Nearest neighbor index is one of the methods of measuring the pattern of feature locations. Ecologists Phillip Clark and Frances Evans' research lead to the nearest neighbor index development in the 1950s. The method was developed to measure patterns in distributions of various plant species. The distance between each feature and its nearest neighbor is calculated then the average, or mean, of these distances is computed. Essentially, the distances between each pair of nearest neighbors are combined then the result is divided by the number of features to obtain the mean distance $\bar{d}_o$ (Equation 1). The index compares the similarities between the mean distance and the expected mean distance for the hypothetical random distribution (Mitchell, 2009).

The mean distance for the observed distribution of features

$$\bar{d}_o = \frac{\sum_i C_i}{n}$$

Measure the distance for each feature's nearest neighbor (C_i), and sum the distances…

…then divide by the number of features

Equation 1. Nearest neighbor mean distance (adapted from Mitchell, 2009)

The nearest neighbor index may either be the difference, $d = \bar{d}_o - \bar{d}_e$, or the ratio, $r = \bar{d}_o / \bar{d}_e$, between the observed and the expected distance (Equations 2 and 3 respectively). If the mean distance of the observed features is less than the mean of the random distribution then the

observed is more clustered than the random distribution. In order to obtain the index, the distance is calculated by subtracting the expected mean distance from the observed mean distance. The difference is zero if the observed and the expected means are equal. Therefore, the observed distribution is a random distribution. If the difference is less than zero, that is negative, the expected mean is greater than the observed mean and the observed distribution is clustered. The opposite is true for a dispersed distribution where the expected mean is less than the observed and the difference is greater than zero (Mitchell, 2009).

The nearest neighbor index as the difference

$$d = \bar{d}_o - \bar{d}_e$$

Subtract the mean distance for an expected random distribution from the mean distance for the observed distribution

The mean distance for the observed distribution of features

$$\bar{d}_o = \frac{\sum_i C_i}{n}$$

Measure the distance to each feature's nearest neighbor (C_i), and sum the distances… then divide by the number of features

The expected mean distance for a random distribution

$$\bar{d}_e = \frac{0.5}{\sqrt{n/A}}$$

Divide 0.5 by the square root of the number of features divided the area

Equation 2. Nearest neighbor index as a difference (adapted from Mitchell, 2009)

In the ratio method, $r = \bar{d}_o / \bar{d}_e$, of the nearest neighbor index calculation (Equation 3), if the means are the same the ratio is one and the distribution is random. If the ratio is less than one so that the expected mean is greater than the observed, the distribution is clustered. In fact, the closer the ratio is to zero the more clustered the arrangement; zero is the value for a completely clustered distribution. In other words, the smaller the average distance between the features are from that of the random distribution, the more clustered. Conversely, if the ratio is greater than one, the expected mean is less than the observed mean and the result is a dispersed distribution (Mitchell, 2009).

The nearest neighbor index as a ratio

$$r = \frac{\bar{d}_O}{\bar{d}_e}$$

Divide the observed mean distance by the expected mean distance for a random distribution

Equation 3. Nearest neighbor index as a ratio (adapted from Mitchell, 2009)

The null hypothesis for testing the nearest neighbor index is that the features are randomly distributed. The Z-score test is calculated via the division of the difference between the observed and the expected by the standard error (Equation 4) (Mitchell, 2009).

The Z-score

$$Z = \frac{\bar{d}_O - \bar{d}_e}{SE}$$

The expected mean distance is subtracted from the observed mean distance…

…and the difference divided by the standard error

Equation 4. The Z-score (adapted from Mitchell, 2009)

The standard error, SE, (Equation 5) quantifies the distribution of mean distances about their average value. It is the equivalent to the standard deviation of the mean distance for all features in the data set divided by the square root of the number of features. A positive Z-score, the observed mean distance is greater than the expected mean distance, denotes a dispersed distribution. A negative Z-score, the observed mean distance is less than the expected mean distance, denotes a clustered distribution. The Z-score would have to be greater than 1.96 or less than -1.96 to be statistically significant at the 0.05 level of significance level (Mitchell, 2009).

The standard error

$$SE = \frac{0.26136}{\sqrt{n^2/A}}$$

0.26136 (a constant derived from the radius of a circle) is divided by…

… the square root of the number of features squared (n^2) divided by the areal extent (A) of the study area

Equation 5. The standard error (adapted from Mitchell, 2009)

Another method for measuring the pattern of feature locations is counting the number of neighboring features within defined distances of each feature, and then totaling the values. To

achieve this, a distance interval is specified and the average number of neighboring features within the distance of each feature is calculated. A distribution is considered clustered if the average number of features at a certain distance is larger than the average concentration of features throughout the study area. In other words, it is clustered if the number of features within a given distance is larger than that of a random distribution. This method is named Ripley's K-statistic after statistician Brian Ripley. It is a univariate, second-order, two-dimensional space analysis of point patterns. The second order term relates to the analysis of all point-to-point distances rather than the mean inter-point distances used in the nearest neighbor, a first-order analysis. The K-function includes all neighbors within the specified distance. K represents the number of distance ranges that will be established around each feature. The maximum distance is determined by calculating half the maximum dimension of the study area. The resulting value is divided by the number of bands stated to calculate the distance intervals. Generally, the greater the amount of bands the smoother the chart curve and the easier it is to identify the distance at which clustering peaks. Eventually, increasing the amount of bands further will no longer provide useful information (Mitchell, 2009; Woodall, 2002).

The K-function is basically a descriptor of the extent to which spatial dependence exists in the distribution of the events. Specifically, the K-function is calculated by finding the distance from each feature location to every other feature location. Surrounding features are counted within the specified distance of the feature. A K-value, K(d), is then calculated at each distance for the number of bands stipulated (Equation 6) (Gatrell, Bailey, Diggle, Rowlingson, 1996; Mitchell, 2009).

In order to determine if a pattern exists, the observed K value at each distance is compared to the expected K value for a random distribution; the random distribution is

calculated given the same area and number of features. K-values increase as distances increase. Therefore, K-values are transformed (Equation 7) so to achieve a reasonable Y-axis chart height for ease of interpretation. The transformation technique used is referred to as the L(d) method in which the square root of the resulting multiplication of the area for the number of features in a certain distance divided by π and multiplied by all the possible number of pairs (Mitchell, 2009).

The value of the K statistic at a given distance (d) $\mathbf{K(d) = \frac{A}{n^2} \sum_{i \neq j} \sum_{j} I_{ij}\ d_{ij}}$

The distance (d) is measured between each target feature (i) and every other feature (j); each distance is multiplied by the weight for the pair (I_{ij}), and all these values are summed ($i \neq j$) means the distance between the target and itself is not included in the sum),,,

… then the result is multiplied by the area (A) divided by the number of features (n) squared

Equation 6. The value of the *K*-statistic at a distance (adapted from Mitchell, 2009)

The L(d) method produces an expected value for any distance, given a random distribution of features, that is the distance (d) itself. The distribution is clustered if the observed L value at a particular distance is greater than the expected value for a random distribution. If the observed value is lower than the expected, the distribution is dispersed. A larger L value denotes a larger number of features at a particular distance and clustering ensues where a peak of these values in the chart occur at that distance. A pattern is statistically significant when the observed distribution falls outside the confidence limits for a random distribution. In order to calculate the confidence limits, x- and y-coordinate values are randomly created and the L values calculated at each distance for that distribution. Since there may be a wide variety of possible values between two random distributions, several iterations of the random distribution can be processed to attain a range of possible L values. A confidence envelope, or confidence interval, is estimated by selecting the highest and lowest value at each distance from these simulations to form the upper and lower bounds of the envelope. A pattern that is a statistically significant cluster, that is the

null hypothesis of spatial randomness is rejected, at a given distance is indicated by an observed L value that exceeds the upper confidence limit. A statistically significant dispersed distribution is indicated by an observed L value that is below the lower confidence limit (Mitchell, 2009; Woodall, 2002).

The value of the L at a given distance (d) $\mathbf{L(d) = \sqrt{\frac{A \sum_{i \neq j} \sum I_{ij}\ d_{ij}}{\pi n\ (n-1)}}}$

The distance (d) is measured between each target feature (i) and every other feature (j); each distance is multiplied by the weight for the pair (I_{ij}), which is one if within the distance and zero if not…

…the distances are summed (excluding the distance between the target and itself) and multiplied by the area (A)…

…then the result is divided by pi times the number of possible point pairs represented as the number of points (n) times the number less one; and the square root is taken

Equation 7. The L(d) transformation method (adapted from Mitchell, 2009)

Features that are neighboring the edge of a study boundary may bias the results of the *K*-function. These features have fewer neighbors, may be at further distances with fewer surrounding points and so are susceptible to edge effects. Edge effects may occur when features outside of the boundary are not included in the calculation even if these are within the specified distance. *K*-statistic calculation methods, such as the inclusion of edge simulation, are available to remedy this effect (Mitchell, 2009; Dixon, 2002).

Ripley's *K* (cumulative pairs over a distance) is a spatial association measure among others such as Getis and Ord's Gi* measure of local clustering (Getis, 2008).

The Gi* statistic is constructed on the premise that a spatial association exists between observations to a distance. This local statistic theory is dependent on a critical distance specification beyond which clustering of high or low values no longer increases. It is inferred then that the spatial association ends at the critical value. A spatial weights matrix defines

important parameters for the calculation of the Gi* (pronounced g-i-star) statistic. It is an essential part of this analysis and is the formal representation of spatial dependence between observations (Getis, Aldstadt, 2003).

Identifying clusters of features with similar values of a particular characteristic involves examining the attribution of each feature and its neighboring features, along with the proximity of these features. A statistical calculation for each point reveals the extent of similarity of nearby feature values for a particular characteristic. These statistical values can be plotted spatially to visually identify the clusters of features with similar values. Mapping the features in this manner provides a statistically sound method for identifying clusters of points with a similar characteristic. It is a determination that the likelihood that a feature with similar values as its neighbors is not simply due to chance (Mitchell, 2009).

In a case where the value of the target feature is a factor in the outcome of a clustered pattern, a Gi* local statistic is most appropriate technique for identifying clusters of similar value, hot spots or cold spots. The Gi* is either based on a neighborhood of feature adjacency or a specified distance. The length used in a distance-based neighborhood is dependent on the researcher's knowledge of the events and their behavior. Distances are characterized as straight-line, Euclidian, or as travel time over a street network or overland (Mitchell, 2009).

A Gi* statistic, $G_i^*(d)$, is calculated by summing the values of the neighbors and dividing by the sum of all the study area features' values (Equation 8). Because a binary weight is used, as either adjacency neighbors or distance neighbors, the characteristic values are multiplied by one for neighbors and zero for others; which is the same as the sum of the neighbors' values. Therefore, only neighbors are included (Mitchell, 2009).

G_i^* for a feature (i), at a distance (d)

$$G_i^*(d) = \frac{\sum_j w_{ij}(d) x_j}{\sum_j x_j}$$

The value of each neighbor (x_j), is multiplied by the weight for the target-neighbor pair (w_{ij}), and the results summed …

…then the sum is divided by the sum of the values of all neighbors (x_j), that is, all features in the data set

Equation 8. Gi* statistic calculation (adapted from Mitchell, 2009)

Feature groupings with high Gi* values denotes a concentration of features with high attribute values, or a hot spot. A cold spot is indicated by groupings of features with low Gi* values. A Gi* value near zero denotes that there is no apparent cluster of values. A lack of feature concentration is a result of surrounding values near the mean or a target point that is surrounded by a mix of high and low values (Mitchell, 2009; Getis, Aldstadt, 2003).

The statistical significance of the Gi* is tested by calculating a Z-score. The Z-score calculation (Z (G_i*)), in this case, is performed by subtracting the expected Gi* for the feature in a random distribution from the calculated Gi* value then dividing the difference by the square root of the variance of all the features within the study extent (Equation 9) (Mitchell, 2009).

The Z-score for G_i*

$$Z(G_i^*) = \frac{G_i^* - E(G_i^*)}{\sqrt{Var(G_i^*)}}$$

The expected G_i* value is subtracted from the observed G_i*…

…and the difference divided by the square root of the variance

Equation 9. The Z-score for Gi* (adapted from Mitchell, 2009)

The sum of the weights for a particular distance divided by the number of features in the study area minus one (Equation 10) results in the expected Gi* (E (G_i*)) for a random distribution (Mitchell, 2009).

The expected G_i* value

$$E(G_i^*) = \frac{\sum_j w_{ij}(d)}{n-1}$$

The weights (w_{ij}) at a distance (d) are summed…

…and divided by the number of features (n), minus one

Equation 10. The expected Gi* value - random distribution (adapted from Mitchell, 2009)

Similar to the Gi* value, a high Z-score for a feature indicates neighbors with high attribute values and a feature with low Z-score value indicates neighbors with low attribute values at a given distance. If the Z-score is near zero, there is no evident cluster of similar values. A statistically significant Z-score is either lower or higher than the confidence limits, that is, falls outside the standard normal distribution; for a 95% confidence level, a Z-score that is either greater than 1.96 or less than -1.96 (Mitchell, 2009).

Gi* results, however, can also be influenced by edge effects. Because the neighborhood is determined either by adjacency or distance, features near the boundary of the study area tend to have fewer neighbors and may, therefore, receive greater importance in the calculation skewing the results. Furthermore, the effect of any outliers in an analysis involving a small number of features, say less than thirty, might produce results that are suspect. A local statistic, such as the Gi*, is intended for use in identifying clusters that have an indeterminate clustering or dispersion pattern throughout the region of study (Mitchell, 2009).

Table 2 is a summary of the three types of spatial analysis discussed and the corresponding values that indicate clustering, randomness, or dispersion of values.

Table 2. Summary of statistically significant spatial patterns at the 95% confidence level

	Nearest Neighbor	Ripley's K-function	Gi* statistic
Clustered: Z-score is	< -1.96	> 1.96	> 1.96 or < -1.96
Dispersed: Z-score is	> 1.96	< -1.96	-
Random: Z-score is	<=1.96 & >= -1.96	<=1.96 & >= -1.96	<=1.96 & >= -1.96

2.6 Shrinking and Swelling Soils Overview

Certain types of soil have a moisture content that can be subjected to significant volume changes. Specifically, fine-grained clay soils have a shrinking and swelling tendency. Swelling, or expansive, soils are composed of clay minerals which attract and absorb moisture. Soil shrinkage occurs mainly on the upper layers of the soil. As moisture content declines, surface tension increases. The result is overall soil volume decline. Once the soil is subjected to moisture, the swelling process begins. The likelihood of shrinkage and/or swelling may be classified as very high, high, medium, and low (Holtz, Kovacs, 1981).

CHAPTER 3
DATA AND METHODS

3.1 Study Area - The Baton Rouge Water Works Company

The Baton Rouge Water Company is located in East Baton Parish but also serves customers in the northeastern part of Iberville Parish, Louisiana. The purity of its water is owed to water drawn from wells in underground rock and sand formations that travels in the geologic subsurface structure from the Vicksburg, Mississippi area.

The first well was drilled in 1889 before the Company became known as The Baton Rouge Water Works Company. Two reservoirs were constructed with a total capacity of 1,325,000 gallons. One of these, the Lula Resevoir, still remains in service. By 1973 the Company had some 47 wells ranging from 1,000 to 3,000 feet in depth. The pipes totaled 982 miles and the average daily pumping rate was 31,885,540 gallons per day (Clayton, 1973).

Today the Company covers 150 square miles with approximately 1,500 miles of main. Serving over 240,000 customers, the Company supplies the area with an average of 55,096,000 gallons of water per day (The Baton Rouge Water Works Company - Report, 2009). Its system is composed of 65 water wells, 39 stations with pumps, 15 house pumps, 12 enclosed storage facilities, 1 station with solely a booster pump, and 1 reservoir (Figure 3).

The service area is composed of pipe segments that can range from 10 feet to approximately 1,000 feet in length. The pipe materials present in the system are polyvinyl chloride, asbestos cement, cast iron, permastrand, steel, ductile iron, tubing, galvanized, polyethylene, and to some extent copper. The change in elevation ranges from about approximately 30 to 60 feet.

The Baton Rouge Water Works nonrevenue water in 2008 totaled 293,983,298 gallons with 12,810,930 gallons attributed to leaks (The Baton Rouge Water Works Company

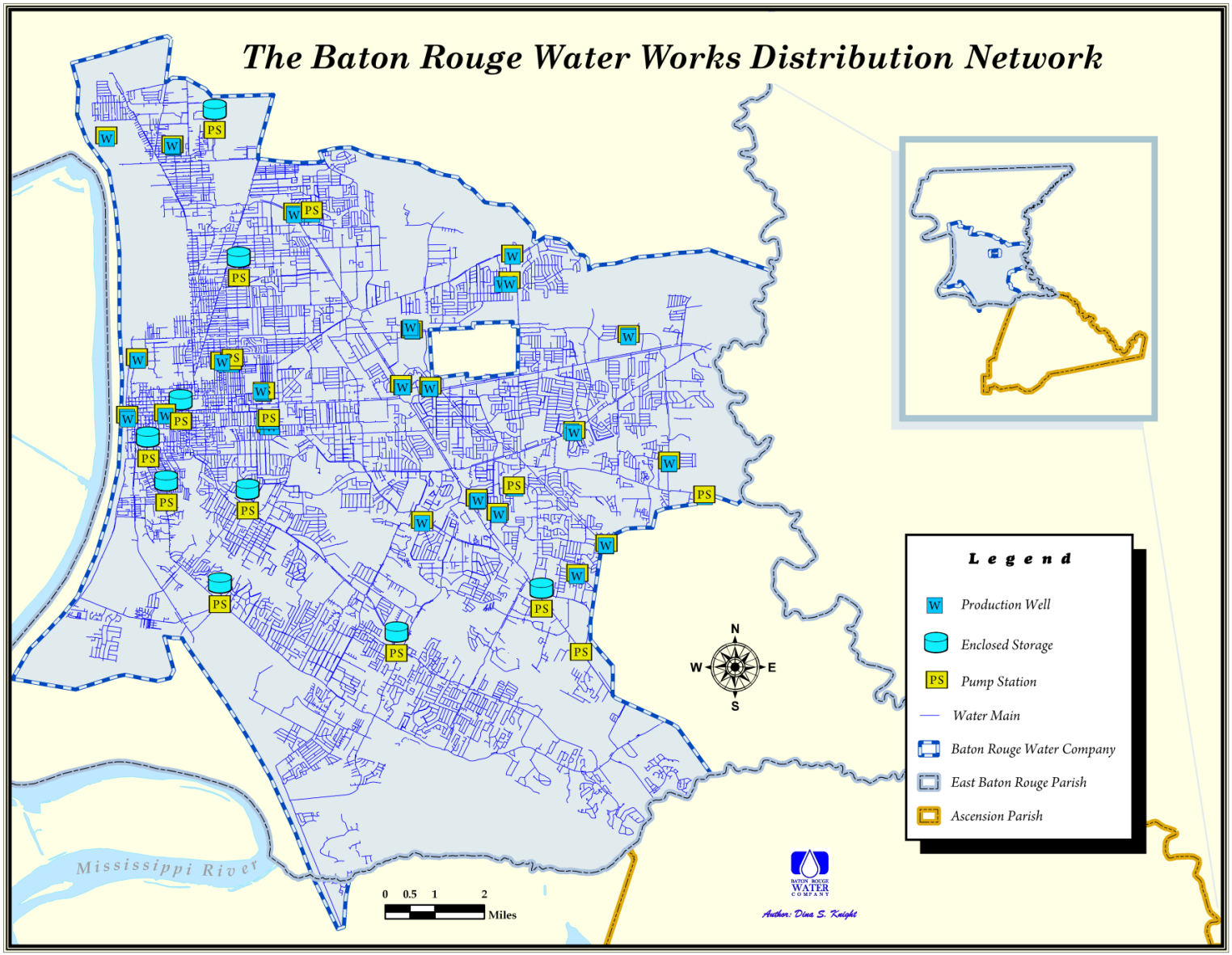

Figure 3. The Baton Rouge Water Works distribution system as of December 3, 2009

Summary, 2008). In 2009 the Company produced 20,069,321,673 gallons of water. The nonrevenue water for 2009 totaled 544,976,471 gallons with 199,598,530 gallons stemming from leaks in the system (The Baton Rouge Water Works Company - Summary, 2009).

3.2 Data Collected for Analysis

The Baton Rouge Water Works Company produces monthly reports on main, hydrant, service, and meter leaks along with other service order quality control issues. The records are maintained for a period of roughly three years after which they are purged. The records contain service address and details on the results of the service order outcome; an example of the data records is shown on Table 3. A report for a period of thirty nine months (October 15, 2006 through January 19, 2010) was generated and the report was thoroughly examined and any unrelated and duplicate records were removed (The Baton Rouge Water Works Company Quality Assurance Log, 2006-2010).

A SCADA system was installed at the Company in the late seventies and updated in the nineties. The SCADA AlarmView component maintains records of station power outages (Table 4). Data was extracted to review thirty nine months of activity (October 15, 2006 - January 19, 2010) (The Baton Rouge Water Works Company, 2006-2010).

Table 3. Quality Assurance Log example entries

Entry Date	Reason	Address	Zipcode	Follow-up
20061015	41	1 Applewood Rd	70808	Repaired 2 1/2" PVC Main
20070111	41	2 Aurora Pl	70806	Repaired 2 1/2" PVC Main
20080731	41	3 Churchill Ave	70808	Repaired 8" CI Main
20080303	42	4 Compton Ct	70809	Repaired Service Line
20090805	42	5 Lee Dr	70808	Repaired 2" GA Main
20100116	40	6 Ardenwood Dr N	70806	Repaired Hydrant

Table 4. Example of the SCADA AlarmView power failure log

Date Time	Company	Name	Outage	Event
02/15/2010 09:31:45	B	I_12	Utility Power	Normal
03/07/2007 14:34:15	B	LULA21	Utility Power	Fail
06/09/2009 15:20:25	B	LULA_E	Utility Power	Normal
03/07/2007 14:34:15	B	PRESCT	Utility Power	Fail
01/22/2007 15:50:27	B	SOUTER	Utility Power	Fail
04/24/2008 06:04:05	B	TEXAS	Utility Power	Normal

3.3 Methodology and Techniques

Cases studies have been conducted to compare simplified and comprehensive surge analysis indicating the need for system-specific analysis. However, to our knowledge no studies have been conducted to actually show the extent of transient wave effect on pipeline damage or to show the relationship in spatial terms.

Transient events caused by pump trips can potentially lead to pipe system damage such that leaks would become evident, and would cluster, in areas in close proximity to pump stations. Leak and station power failure activity was reviewed and then analyzed to discover whether such a relationship exists in this study area; the entire spatial and frequency analysis, spatial data preparation, manipulation, and graphing components of this study were conducted using ESRI ArcGIS software.

First, a report containing main, hydrant, service, and meter leaks for the thirty nine month period was examined and any unrelated and duplicate records removed. The main, hydrant, service, and meter leaks were then geocoded in order to conduct spatial distribution analysis. The geocoding resulted in 99% address matching (Figure 4); out of 5,263 addresses, 5,236 matched, 27 tied and 11 were unmatched.

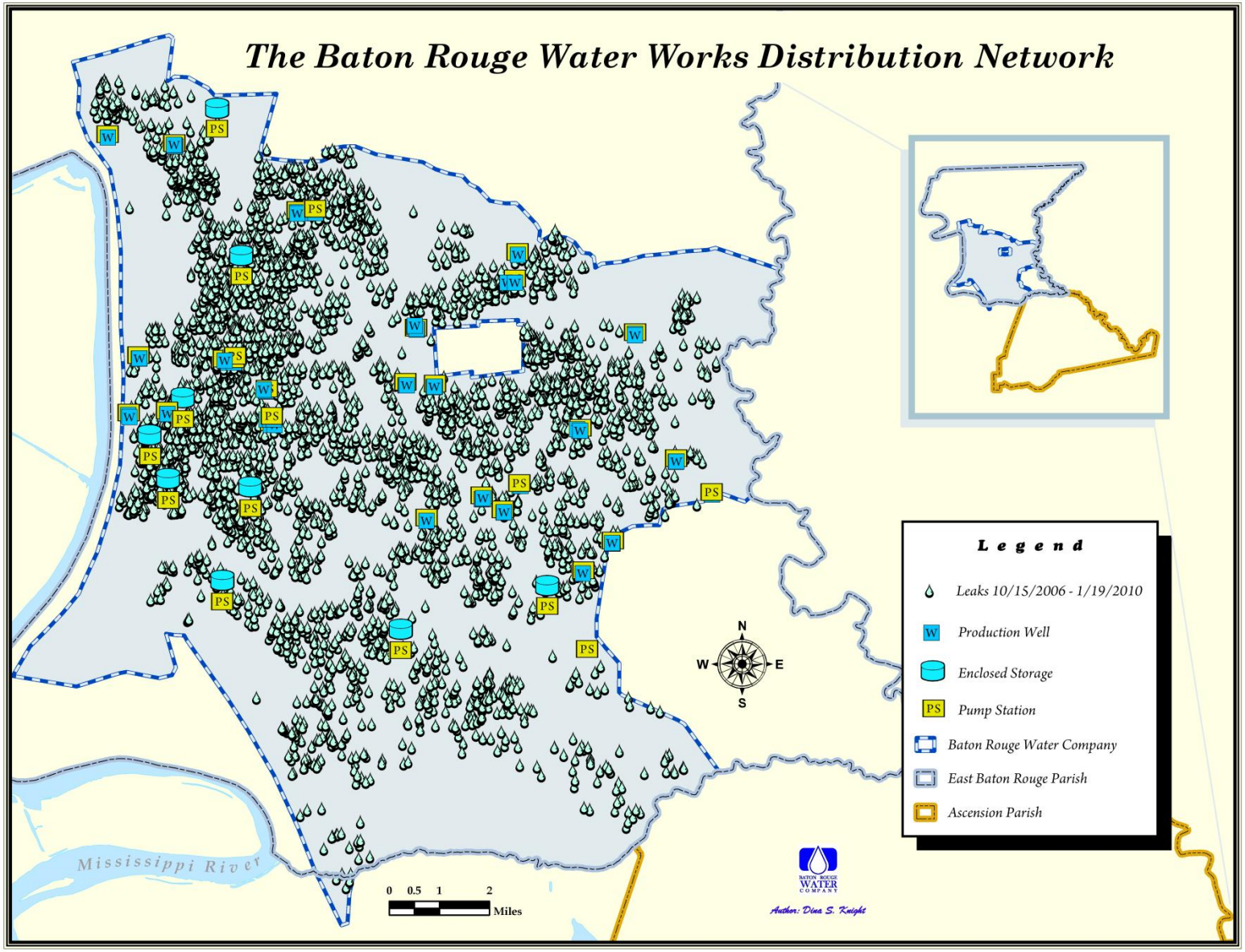

Figure 4. Geocoding results

Initially, the raw geocoded data was processed with the average nearest neighbor distance (Equation 1, Section 2.5) spatial statistic to determine whether spatial clustering is evident. The average nearest neighbor statistic calculates the average distance from a feature's own location to its nearest neighbor. The Manhattan distance approach was chosen as the method of distance calculation since water mains follow a city block model; as opposed to Euclidean, straight line, method of distance calculation which is appropriate for continuous data. In addition, the study area size was defined to 5,664,423,037 square feet in order to more accurately represent the extent of the study area and to ensure that every feature in the study area is captured during this analysis. This method of analyzing patterns is based on inferential statistics providing a broad measure of spatial pattern. The null hypothesis for the average nearest neighbor distance spatial statistic assumes that the features are randomly distributed or lack spatial pattern. Nearest Neighbor ratios below one indicate clustering.

Additional processes were applied to the data in preparation for the hot spot analysis (G_i* local statistic – Equation 8, Section 2.5). First, the geocoded data was rendered to combine coincident features. A new attribute (field) is created in this process to store the number of coincident features. Then, a spatial weights matrix file was created using a fixed distance and, since water mains follow a city block model, the Manhattan method of distance calculation. Then, the multi-distance spatial cluster analysis (Ripley's K-function statistic – Equation 6, Section 2.5) was employed to determine the distance, or distances, that exhibit clustering. The multi-distance function assumes the pattern of weighted points is not significantly more clustered than the underlying features.

Twenty bands were used to provide an adequate level of distance intervals for proper identification of the distance at which clustering peaks. Ninety-nine permutations were used for

the confidence envelope calculation; the choices include 9 simulations for a 90% confidence level, 99 simulations for 99% confidence level, and 999 simulations for 99.9% confidence level. The weight attribute containing the number of features at each location in the rendered layer was used for the multi-distance analysis for a proper feature weight assessment. The simulate outer boundary values method of boundary correction was chosen to resolve any underestimates that may occur near the edges of the study area boundary; lack of neighboring points can skew the data. This method mirrors points across the study area boundary so that edge points will have more truthful neighbor estimates. Other methods include, reduce analysis area, which is not available when a study boundary file is used, and the Ripley's edge correction, which is appropriate for very square or rectangular study areas. Additionally, since the K-function is sensitive to study area size, a boundary layer was used to more accurately represent the extent of the study area. The K-function is an effective means to summarize spatial dependence of different scales or distances (Bailey, Gatrell, 1995).

A hot-spot analysis was performed using the rendered dataset, the spatial weights matrix file, and the distance identified in the multi-distance spatial cluster analysis that was most pronounced and statistically significant. The weight matrix used in the hot spot analysis was computed by using the Fixed Distance Band method of conceptualization of spatial relationships. This method was applied so as to define whether neighboring features which fall inside the specified critical distance receive a weight of 1, and exert influence on computations for the target feature, or a weight of zero, falling outside the critical distance, and have no influence. The threshold distance (critical distance) for the fixed distance band is the significantly-clustered distance result from the K-function analysis. Again, the Manhattan method of distance calculation was applied to the matrix as main vectors follow a city-block configuration.

Finally, eight neighbors were selected as the number of neighbors to consider in the calculation so that each feature will have at least this many neighbors. This technique ensures that, when necessary, at least the requested amount of neighbors are used; in this scenario the threshold distance may be temporarily extended.

The hot spot analysis should provide a better understanding of the leak concentrations. In the hot-spot analysis a Getis-Ord Gi* statistic is calculated for each instance or event. A Z-score and p-value is computed for each event demonstrating the spatial distribution and clustering of high and low values. An event that is a statistically significant hot-spot has a high value and is surrounded by events with high values. In essence, the local sum for an event and surrounding neighbors is evaluated relative to the sum of all events. If the local sum is considerably different from the expected sum and the difference is too great to be the result of random chance, then a statistically significant Z-score is assigned to that event. Large positive Z-scores with small p-values (less than or equal to 0.05) indicate intense clustering of high values, hot spots, and smaller Z-scores with small p-values indicate clustering of low values or cold-spots.

Leak time of occurrence and frequency was examined and compared with the power failure temporal and frequency data over a period of thirty-nine months. The SCADA system provided the data containing station activity. The temporal and frequency data for leaks and power failures in areas demonstrating a concentration of leaks near a pump station were graphed. The goal was to uncover a close relationship between frequency and time of leaks with the frequency and time of power failures.

Furthermore, a comparison of the resulting leak clusters near stations was made with hydraulic surge models of the same areas. The model was prepared and conducted by Chris Morris, Hydraulic Systems Analyst at Owen & White Inc., Consulting Engineers.

The transient modeling process begins with a steady-state hydraulic procedure in WaterCAD (Bently Systems, Inc.). A peak-hour customer demand of 0.65 gpm (gallons per minute) with a combination of wells, booster pumps, and booster stations is established to fulfill the demand and maintain the system pressures within normal operating ranges; A total of 104,190 gpm or 150 MGD (millions of gallons a day) flow rate. A sub-model of the area of interest is extracted after the steady state is achieved. The sub-model is then exported to a file containing the elements and its attributes necessary for the transient analysis in the Surge2010 software (KYPipe LLC). The newly imported data is compared to the WaterCAD main water system configuration for accuracy and any loss of information during the transfer process. Additionally, modifications to run the steady-state simulation are necessary to account for demands and inflow from lines outside of the sub-model. Other information such as pump characteristics (speed, head, flow inertia, efficiency, and torque – as a function of flow and speed) are also entered into the model for the Surge2010 simulation. Another component of the surge model is the wave speed of certain piping materials. In the areas of interest, a speed of 3600 ft/s was assigned to ductile iron and 2000 ft/s for PVC pipe. Finally, a transient surge simulation is performed. The simulation begins with a steady-state condition for five seconds followed by a pump failure. The resulting output comprises of maximum and minimum pressures that will reveal areas requiring investigation. A profile of questionable areas may be generated to display the pipeline, hydraulic grade line, maximum and minimum pressures in order to visualize transient wave propagation (Morris, 2011).

CHAPTER 4
RESULTS AND DISCUSSION

4.1 Nearest Neighbor Analysis

The results of the nearest neighbor procedure demonstrated clustering of the leak events with a ratio of 0.52 and a -66.39 Z score value (Figure 5); unlike the hot spot analysis, this method provides resulting statistics and does not provide an output of the data that can be mapped. At the significance level of 0.01, we reject the hypothesis that this distribution is random and conclude that the leak distribution is clustered. Consequently, further analysis was performed to discover the extent of clustering.

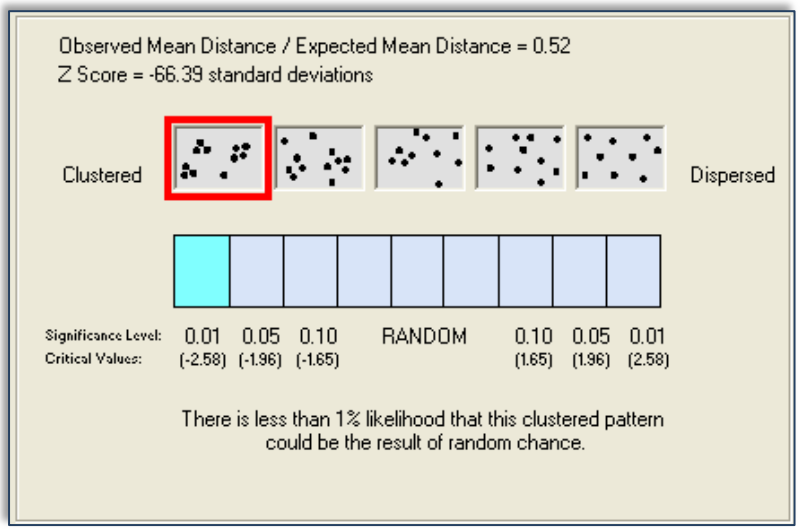

Figure 5. Average Nearest Neighbor Distance results

4.2 Ripley's K Function

Subsequently, the multi-distance spatial cluster analysis (Ripley's K-function) was performed to explore at which scale or scales clustering is occurring and to later apply the distance of interest to the hot spot analysis. The results of the analysis show, on 99 simulations (99% confidence level), that clustering is most pronounced and statistically significant at 6,389 feet (1.21 miles) (Table 5).

The distance correlated with largest difference between the expected and the observed values indicates the distance in which clustering is most pronounced. Positive DiffK values indicate clustering and are statistically significant if the ObservedK values fall outside the confidence envelope; negative DiffK values that fall outside of the confidence envelope indicate statistically significant dispersion. Figure 6 illustrates the distances of the ObservedK (red line) associated with the positive DiffK values, demonstrating clustering, are above the ExpectedK (blue line). Conversely, the negative DiffK values indicating dispersion are below the ExpectedK. The highest DiffK positive value (6,389 feet) is the peak of clustering and will be used in the hot-spot analysis.

Table 5. Multi-Distance Spatial Cluster Analysis (Ripley's K-function) results

ExpectedK (miles)	ExpectedK (feet)	ObservedK (feet)	DiffK (feet)	LwConfEnv (feet)	HiConfEnv (feet)
0.20	1064.75	1562.83	498.08	1510.96	1548.48
0.40	2129.50	2799.79	670.29	2736.66	2783.82
0.60	3194.26	3957.20	762.95	3881.34	3949.50
0.81	4259.01	5072.37	813.37	4989.43	5075.21
1.01	5323.76	6171.65	847.89	6068.98	6171.16
1.21	6388.51	7250.25	861.74	7123.28	7245.71
1.41	7453.26	8292.12	838.86	8148.83	8282.54
1.61	8518.01	9290.65	772.63	9140.32	9281.15
1.81	9582.77	10255.90	673.17	10097.10	10250.50
2.02	10647.50	11205.90	558.34	11032.00	11197.10
2.22	11712.30	12137.80	425.55	11952.30	12125.00
2.42	12777.00	13032.40	255.38	12839.00	13016.80
2.62	13841.80	13895.00	53.26	13702.80	13885.00
2.82	14906.50	14747.80	-158.69	14554.90	14735.10
3.02	15971.30	15586.70	-384.61	15392.70	15576.20
3.23	17036.00	16415.10	-620.97	16218.90	16409.90
3.43	18100.80	17228.70	-872.12	17032.40	17225.90
3.63	19165.50	18024.60	-1140.93	17825.30	18024.50
3.83	20230.30	18805.90	-1424.35	18601.50	18806.80
4.03	21295.00	19586.20	-1708.86	19373.20	19591.50

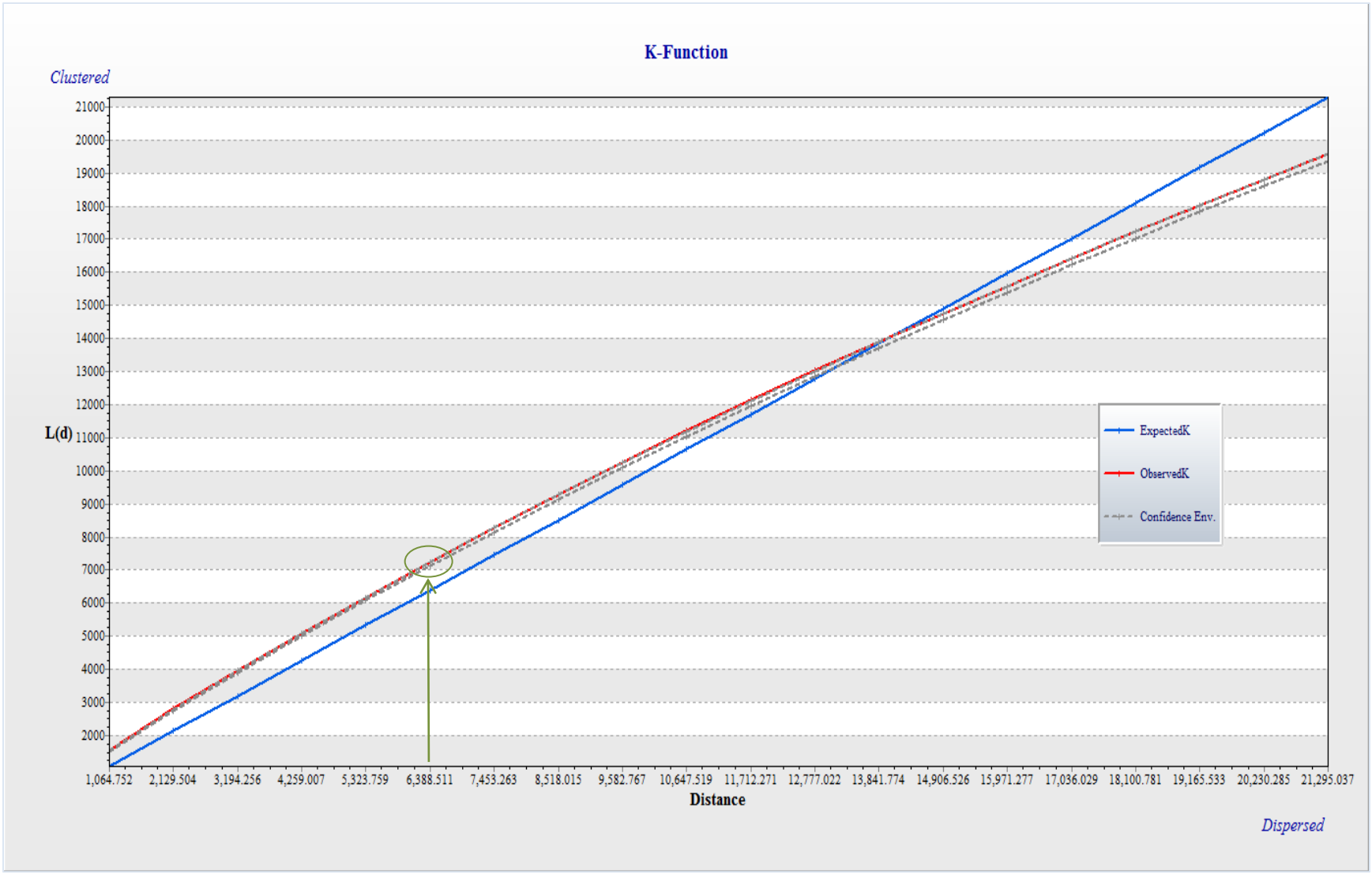

Figure 6. Multi-Distance Spatial Cluster Analysis results

4.3 Gi* Local Statistic

The resulting distance value from the K-function analysis, 6,389 feet, was then applied to the hot spot analysis. As previously mentioned, this analysis was performed using the rendered dataset and a spatial weights matrix file containing the Fixed Distance Band method of conceptualization of spatial relationships, the threshold distance (6,389 feet), the Manhattan method of distance calculation, and eight as the number of neighbors to consider in the calculation so that each feature will have an adequate amount of neighbors.

The results of the hot spot analysis reveals that statistically significant Z-scores are higher than the confidence limits, that is, fall outside the standard normal distribution with a 95% confidence level; Z-scores of feature locations are greater than 1.96 with a 95% confidence level exhibiting clustering of events. Consequently, two main station locations are surrounded by high activity of leaks (Figure 7). The Prescott and the Texas tank stations. The characteristics of these two locations are summarized as on Table 6.

Table 6. Characteristics of Prescott Road and Texas Street

Prescott Road	Texas Street
8” suction, 6” & 16” CI discharge	8” suction, 6” & 16” CI discharge
16” & 12” CI, 8” PVC distribution lines	Into 16” AC distribution line
Pump bypass, 6” check & 10” altitude valve	Pump bypass, 6” check &12” altitude valve
Overhead tank, no wells	Overhead tank, no wells
Velocity: 1.36 fps	Velocity: 1.76 fps
15 HP/1770 RPM Booster pump	20 HP/1775 RPM Booster pump
Output: ~ 850 GPM	Output: ~1,100 GPM
Distribution lines 59% CI, 21% PVC	Distribution lines 52% CI, 21% PVC
Infrastructure age: 40-50+ years old	Infrastructure age: 40-50+ years old

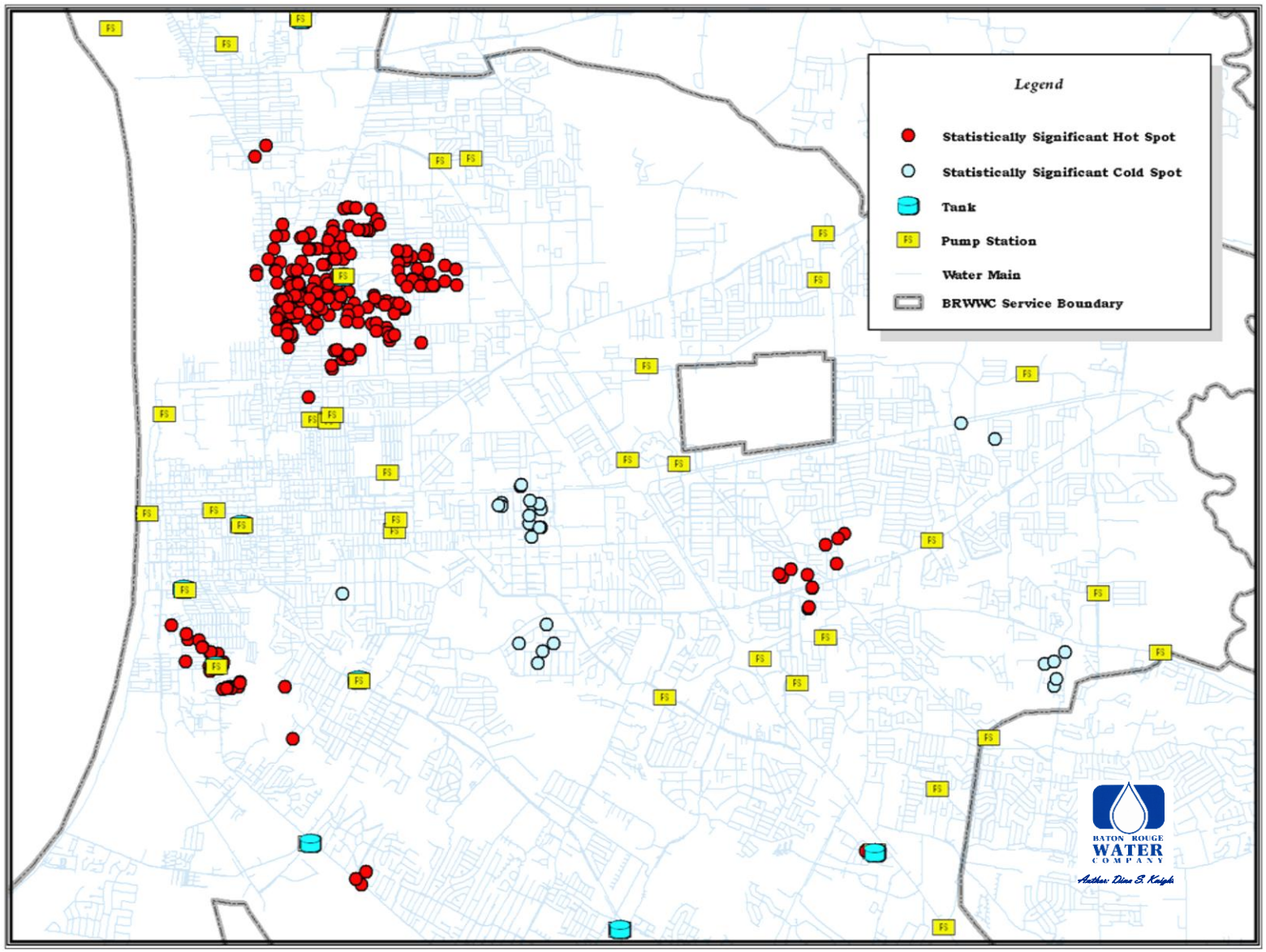

Figure 7. Hot spot analysis results

These stations share similar characteristics. Both of the stations are comprised of overhead tanks, booster pumps, pump bypass lines, altitude valves, and, among other elements, contain the oldest infrastructure in the Baton Rouge Water Company's system. Similarly, the majority of pipe material for both stations consists of cast iron and PVC. Cast iron and PVC are pre-disposed to possible transient wave effect damage. While cast iron is susceptible to breaks from high pressure spikes, PVC is prone to collapse under vacuum pressures.

4.4 Frequency and Temporal Evaluation

To further scrutinize whether the concentrations of breaks in these two areas are due to repeated power failures, a frequency of power failure events was generated for all of the stations in the system (Table 7). Surprisingly, Prescott Road and Texas Street do not have the highest power failure rate. As a comparison, the four stations with the highest frequency of power failures are shown on Table 8. These stations exhibit quite differing characteristics to those of Prescott Road and Texas Street; the stations are I-12, Lula 21 and East (combined due to their proximity to one another – a few hundred feet) , and Souter Drive. However, the Texas Street tank station had forty-two failures and the Prescott station had twenty-six failures in the thirty-nine month period of the study. The amount of failures still warrants closer investigation. Figure 8 displays the location of the stations along with the leak hot spots and the frequency of power failure values.

Next, the power failure and leak events were analyzed for coincidence of leaks and power failure time of occurrence. The simplest and most direct method of comparing these incidents is by plotting the values. Graphs were generated for Prescott Road and Texas Street and are shown on Figures 9 and 10 respectively. A close inspection of these graphs reveals that no evident

Table 7. Power failure frequency by station

Frequency	Site Name
117	Souter Drive
106	I-12
88	Lula East
68	Lula 21
58	North 45th
52	Briarwood Booster
49	Ridgecrest
48	Lafayette
45	Highland Road
45	Lula West
42	Bankston
42	Texas St
39	Government South
37	Government North
…	…
26	Presscott Rd
…	…

Table 8. Characteristics of stations with the highest number of power failures

I-12	Lula 21 & Lula East	Souter Drive
16” DI production discharge	10” CI, 16” CI & 18” ST	12” to 24” DI
Into 12” PVC distribution	Into 12” CI, 16” AC	2-24” DI. to 12” PVC
Air release	Air release	Air release
No overhead tank, 3 wells	No overhead tank, 2 wells	No overhead tank, 6 wells
7 fps	3.13, 2.53 fps	3.28 fps
200 HP: 1800 RPM pumps	150-200 HP: 1175-1780 RPM	200 HP: 1760-1800 RPM
~ 4,400 GPM (1-2 pumps on)	~ 1,100, 2,000 GPM (1-2)	~ 5,000 GPM (3)
34% AC, 30% CI, 29% PVC	57% CI, 18% PVC, 13% GA	50% CI, 25% AC, 11% PVC
Infrastructure 30-35 yrs old	40-50+ yrs old	30-40 yrs old

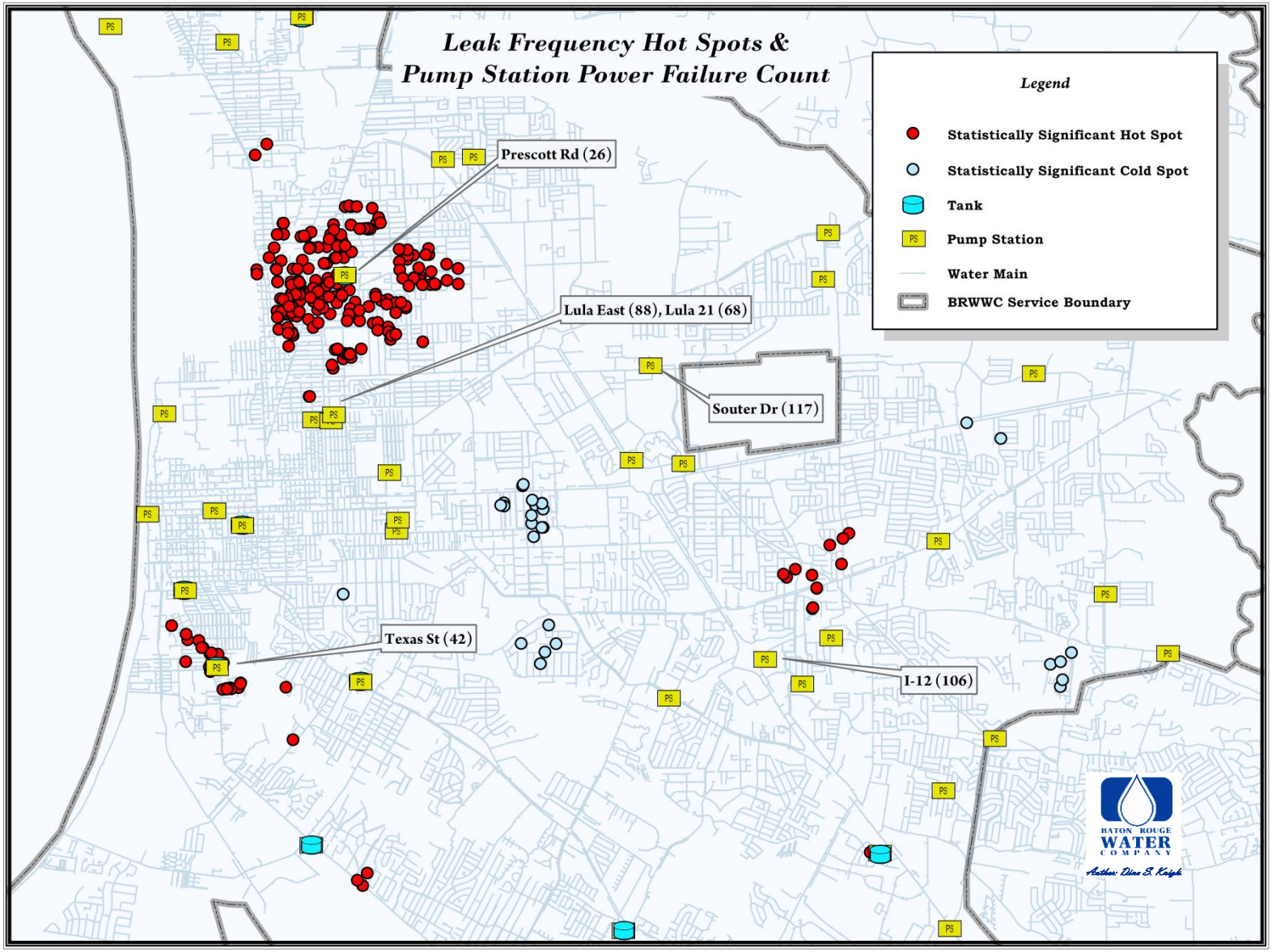

Figure 8. Hot spot analysis results and station power failures

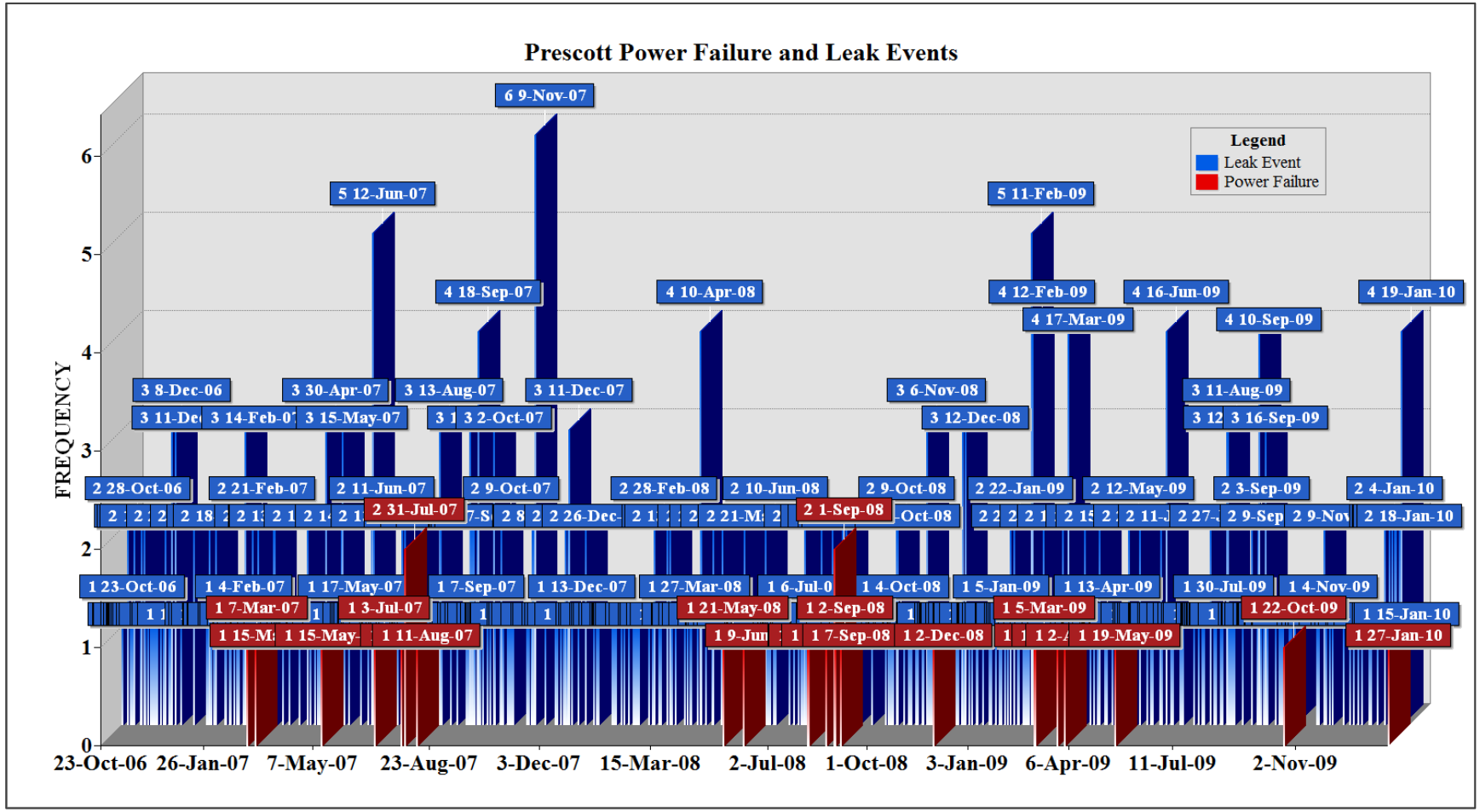

Figure 9. Prescott Road station graph

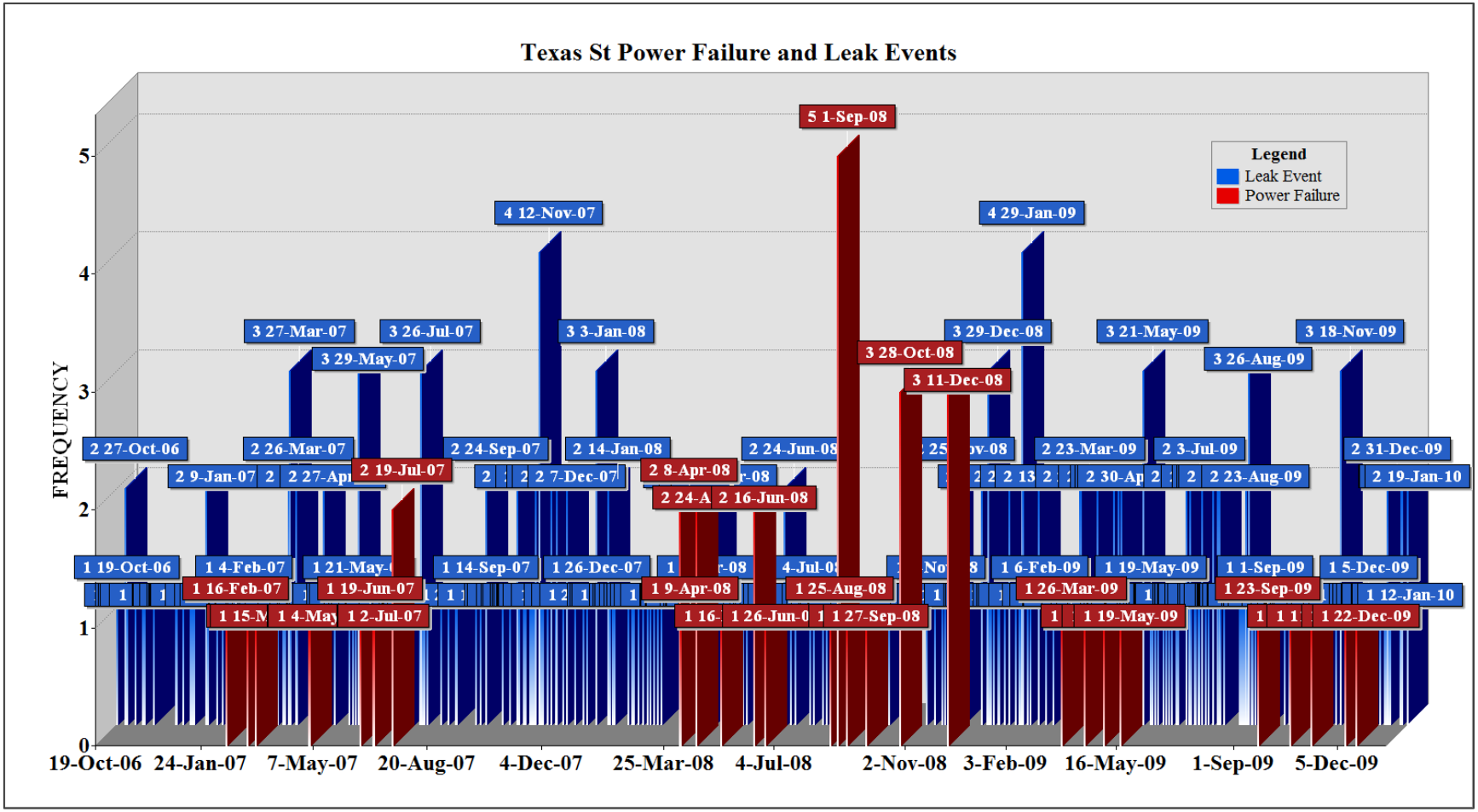

Figure 10. Texas Street station graph

relationship exists. The times of power failure occurrences are not followed by a noticeable increase in leak events in the days and few weeks that follow. The leak events time of occurrence seemingly form concentrations much later than would be the case for making the relationship. Leak events must appear within days or a few weeks of a power failure to merit theorizing a temporal relationship.

4.5 Hydraulic Surge Modeling

The hydraulic surge model for the Prescott Road tank station was simulated using a tank level at 75% (190.15 feet of elevation) and a booster pump output of 1440 gpm (gallons per minute) at 30.2 feet of head. This tank has a capacity of 500,000 gallons and sits at a ground elevation of 56.9 feet. The elevation to the bottom of the bowl is 163.9 feet and 198.9 feet to overflow. The Texas Street tank station was simulated using a tank level at 75% (177.62 feet of elevation) and a booster pump output of 1380 gpm (gallons per minute) at 45.8 feet of head. This tank has a capacity of 1,000,000 gallons with a ground surface of 27 feet. The elevation to the bottom of the bowl is 143.5 feet and 189 feet to overflow (Morris, 2011).

The hydraulic sub-model used for the Prescott Road and Texas Street tank stations simulations are shown on Figures 11 and 12, respectively. The results of the modeling reveal that the lowermost pressure that is reached following a pump trip simulation is 48.7 psig (pounds per square inch) at 6.7 seconds at junction 502 (Figure 13) for the Prescott tank site (Figures 15 and 17). The lowermost pressure reached is 42.6 psig at 8.7 seconds at junction 3220 (Figure 14) for the Texas tank site (Figures 16 and 18). Sub-atmospheric pressures of -14 psig and below must be achieved for cavitation to occur and for possible pressure spikes, which may follow, to arise.

The steady-state HGL (hydraulic grade line) of the simulations, along with the pipeline profile, were diagrammed from the booster pump to the junction where the lowest pressures are

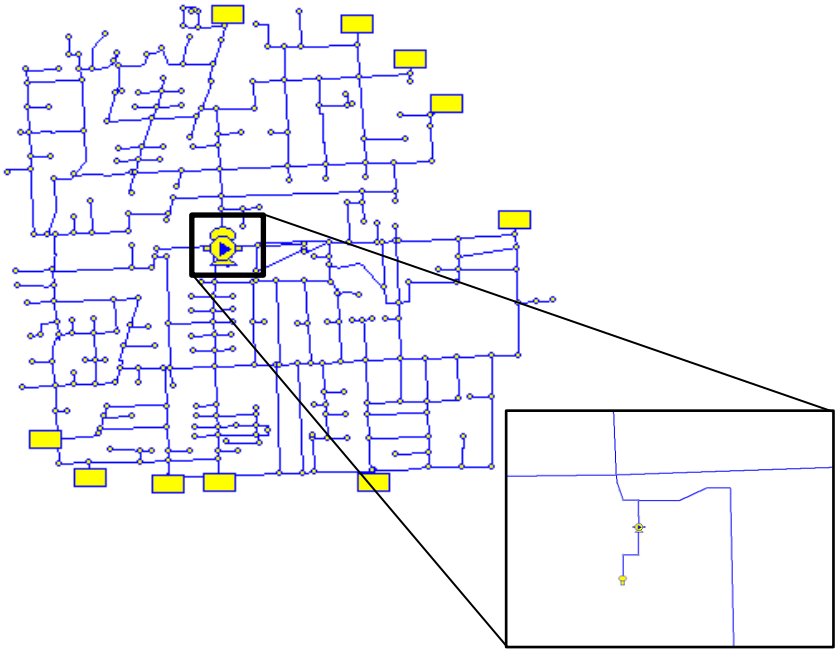

Figure 11. Prescott Road sub-system (Morris, 2011)

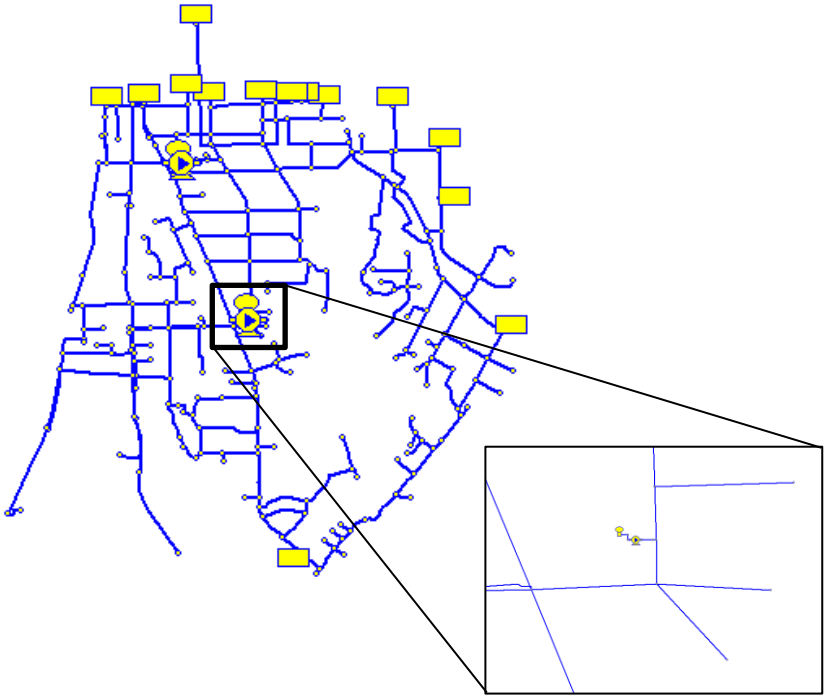

Figure 12. Texas Street sub-system (Morris, 2011)

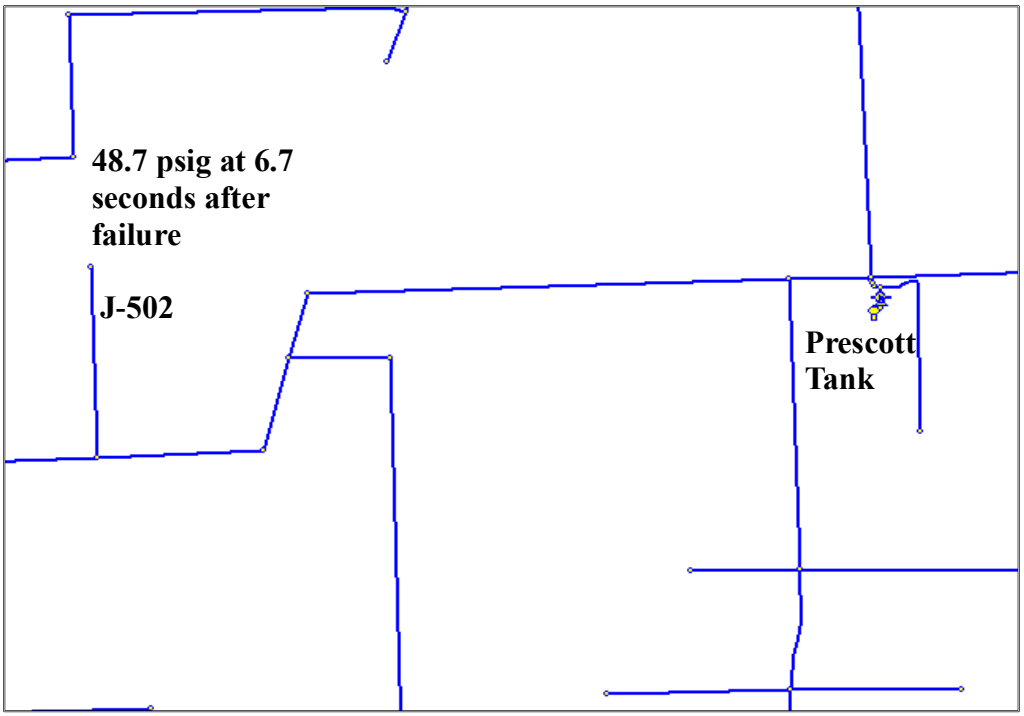

Figure 13. Minimum pressure reached at Junction 502 (Morris, 2011)

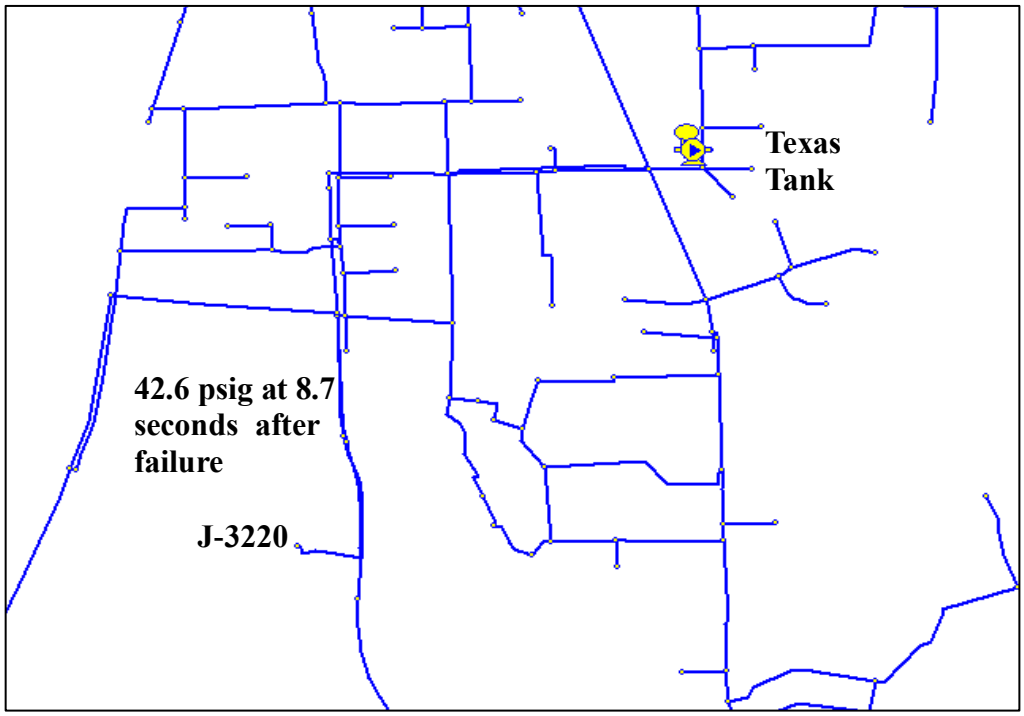

Figure 14. Minimum pressure reached during at Junction 3220 (Morris, 2011)

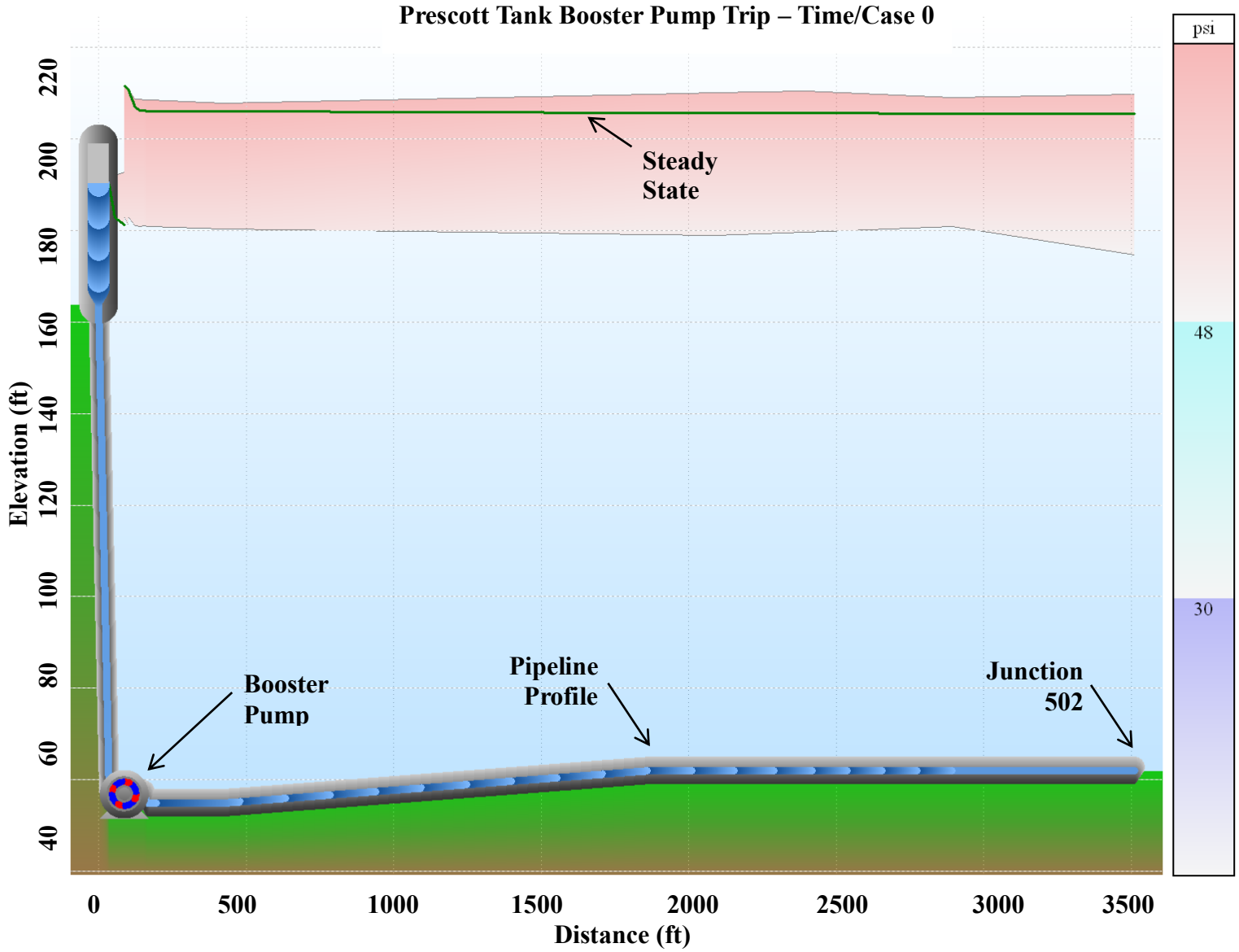

Figure 15. Steady-state HGL for Prescott Road simulation (Morris, 2011)

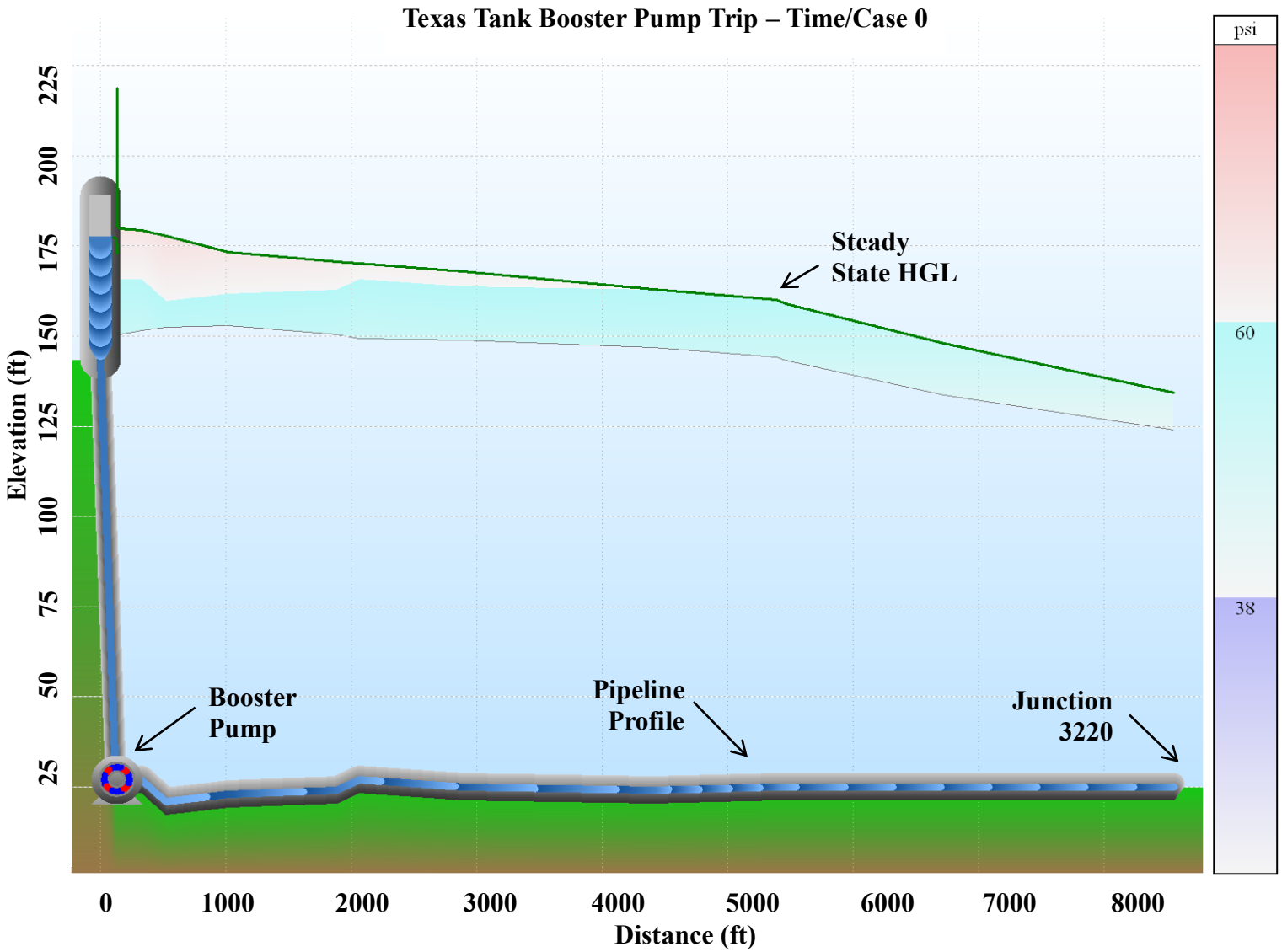

Figure 16. Steady-state HGL for Texas Street simulation (Morris, 2011)

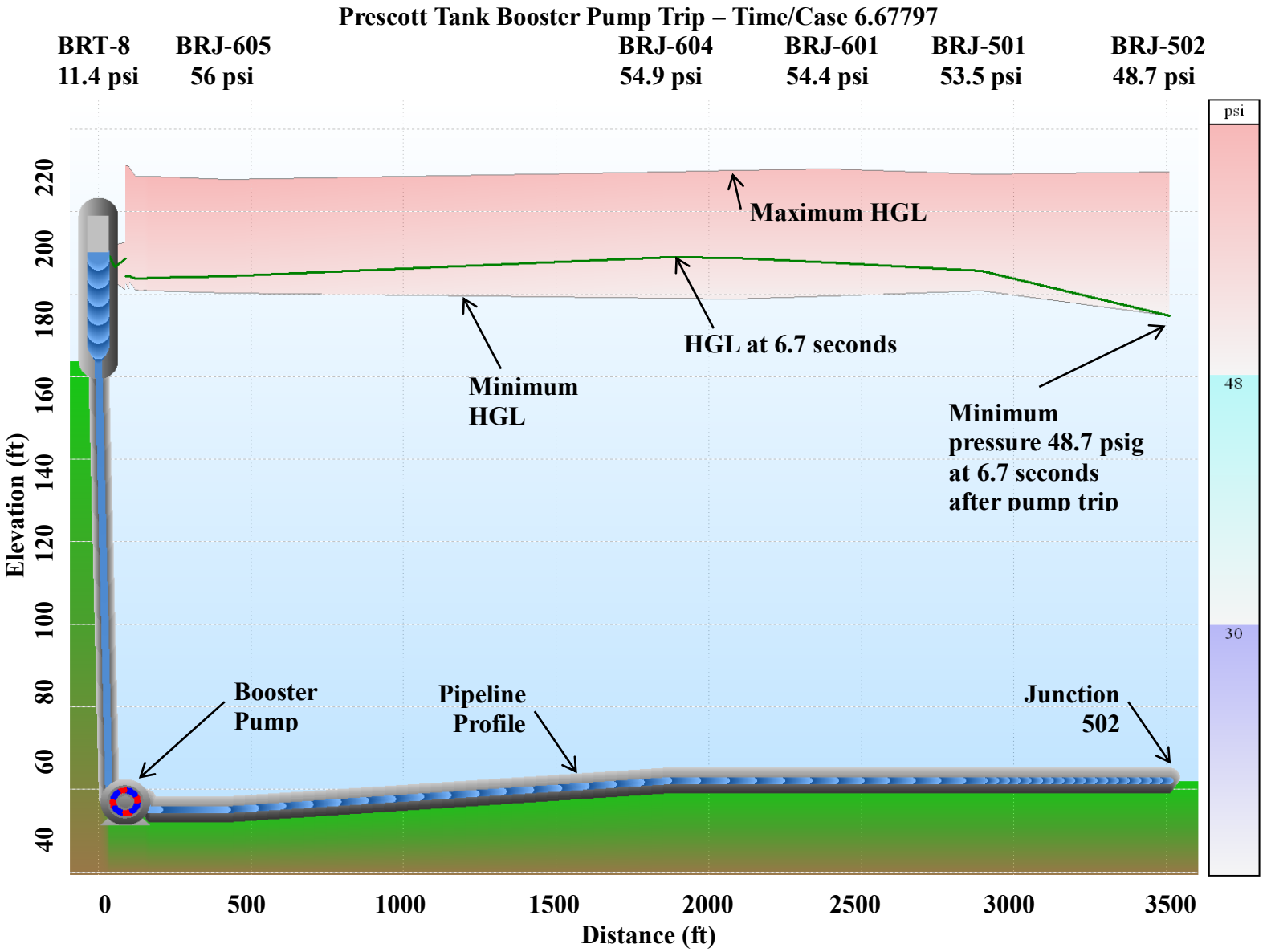

Figure 17. Lowermost pressure at 6.7 seconds for the Prescott Road simulation (Morris, 2011)

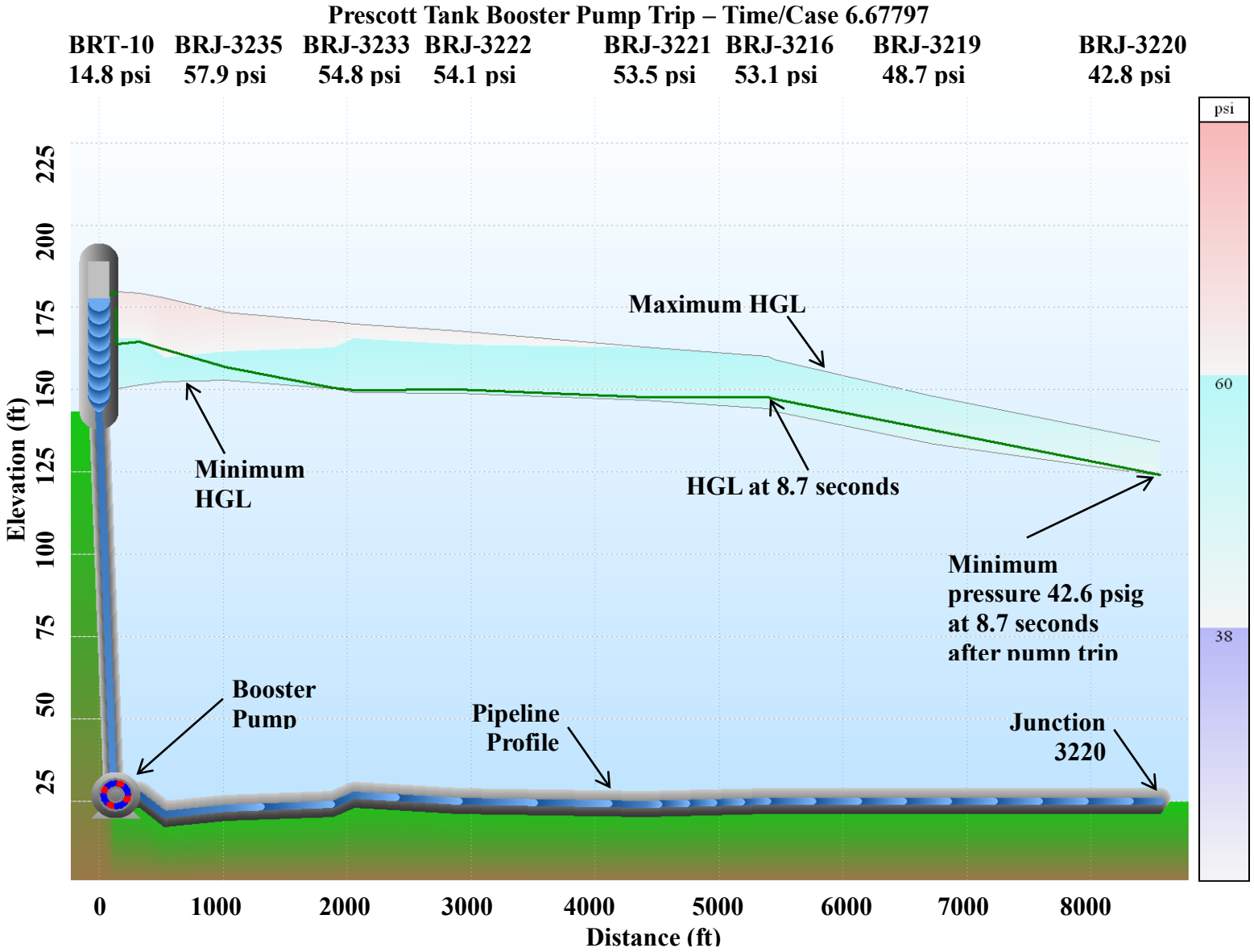

Figure 18. Lowermost pressure at 8.7 seconds for the Texas Road simulation (Morris, 2011)

realized for the Prescott Road and Texas Street tank stations (Figures 15 and 16, respectively); HGL = Z + P/γ where Z is the elevation above the datum, P is the pressure and γ is the weight of the fluid. In a pressurized water environment, the HGL is the level to which water would rise in a vertical tube at any given location along the main. Diagrams follow (Figures 17 and 18) illustrating the minimum HGL, the maximum HGL, and the extent of pressure fluctuations during the simulated pump trip; the gray lines are the bounds for the lowest and highest pressures that are reached during the simulated pump trip event (Walski, Chase, Savic. 2001).

Clearly, no apparent relationship can be presumed of the concentration of leaks near the Prescott Road and Texas Street and power failures events.

4.6 Other Factors Influencing Breaks

The results of this study have shown a concentration of leak events surrounding two stations. These concentrations lack a strong relationship with the power failure events. Therefore, other factrors must be causing these leak incident clusters. Prospects, other than transient events, may include soil shrink and swell and corrosion effects on mains of certain material (Figure 19- steel (ST), ductile iron (DI), asbestos concrete (AC), polyvinyl chloride (PVC), and galvanized (GA)).

	ST	DI	CI	AC	PVC	PE	GA
Collapse under vacuum pressures:	✓*			✓	✓	✓	
Breaks from high pressure spikes:		✓	✓	✓			
Breaks from Shrink and Swell:			✓	✓			
Corrode:	✓	✓	✓				✓

* Thin steel

Figure 19. Pipe material susceptibility

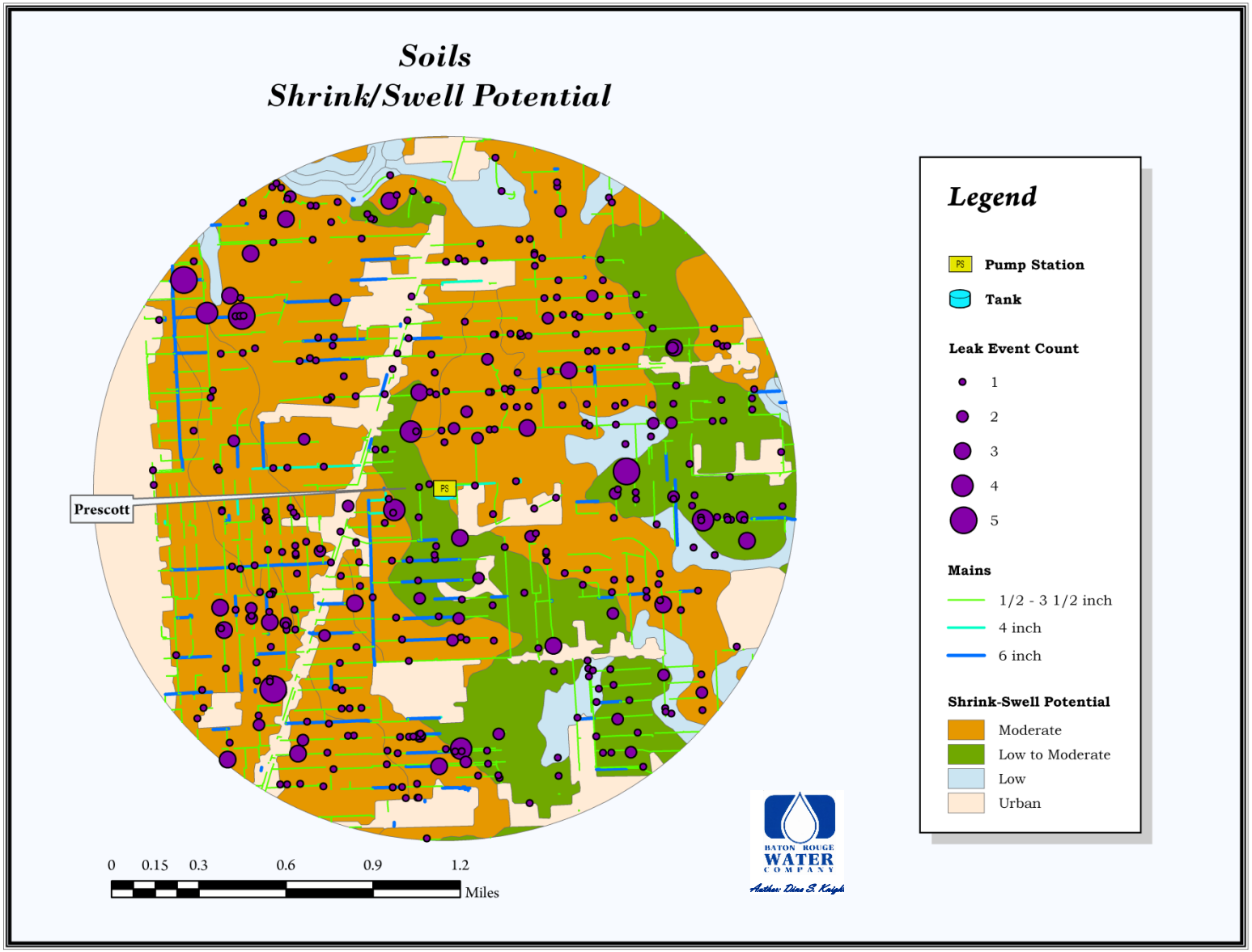

Figure 20. Prescott Road's shrink and swell potential

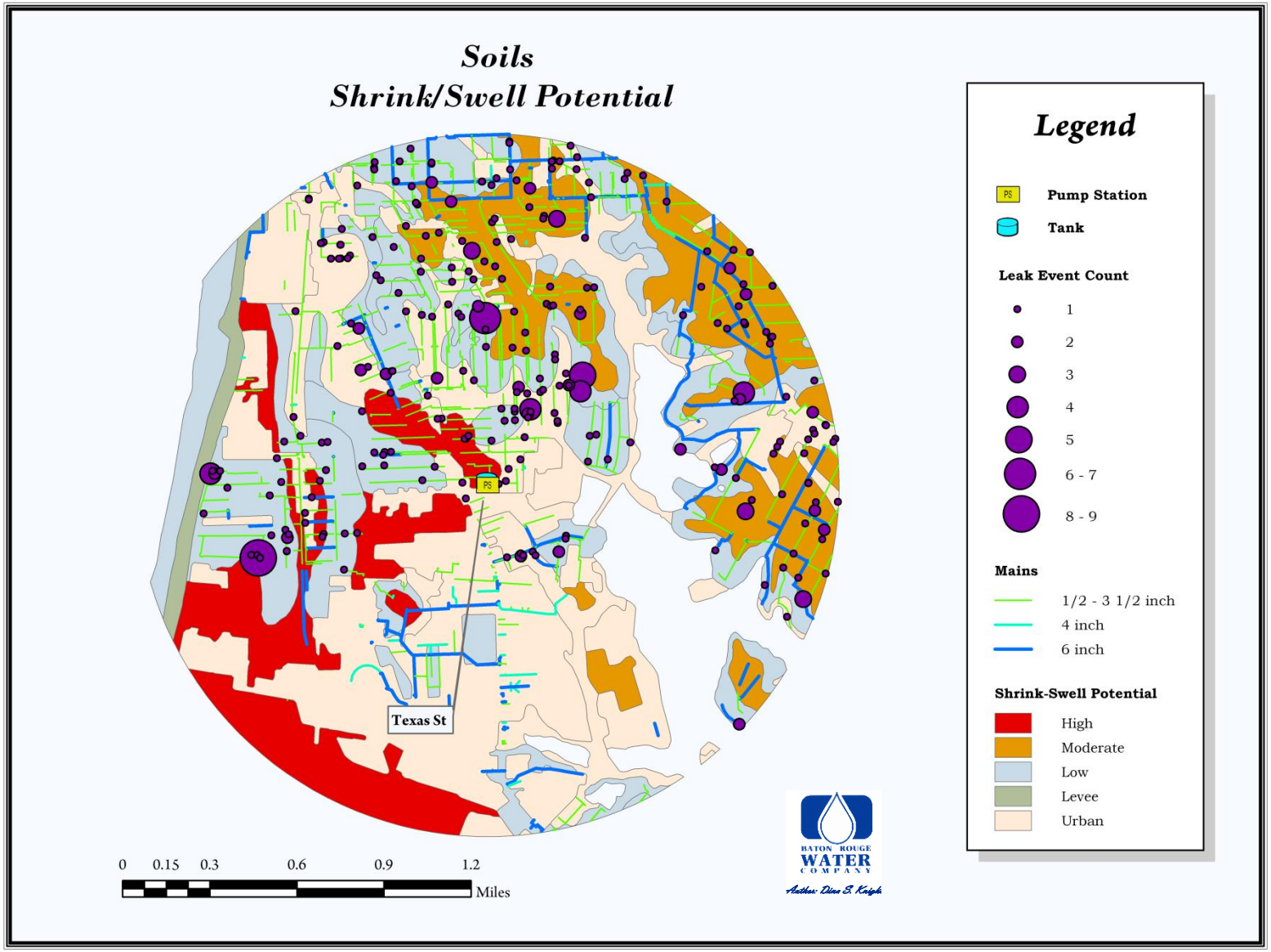

Figure 21. Texas Street's shrink and swell potential

Using data from the USDA Natural Resources Conservation Service, Soil Survey Area Version 7 (02/09/2010), Component Text data and corresponding digital spatial polygon soil data, the areas were mapped to assess the possibility of shrink and swell (Figures 20 and 21).

The classification for probable expansion estimations range from very-high to low. Generally, mains of smaller diameter, mainly of four- and six-inch, tend to be more vulnerable to shrink and swell conditions that fall under the very-high category. Prescott's surrounding area is composed of soils that fall into low to medium classification indicating that shrink and swell is not an issue of great concern. The Texas tank station has some areas of shrink and swell classified as high. Nevertheless, the majority of this classification is either outside of the water system or lacks high concentrations of leak events (Holts and Kovacs, 1981; Owen, pers. comm.).

The Baton Rouge Water Works Company has a system comprising of several water sources (tanks and wells) that provides a continuous supply and flow of water. This characteristic may protect it, to some extent, against transients initiated by power failures (pump trips). In the unlikely event that several pumps lose power at the same time along with the failure of power back-up systems, a transient can generate. Additionally, other transients instigated by rapid valve closure or opening, operational starting and stopping of pumps, tank water level drop, tank pressure change, flushing of hydrants, change in demand, main breaks, regulator and check valve activity may cause damage to a water system's pipes, fittings, and valves. The Company's system has experienced damage from rapid valve closure, flushing of hydrants, and main breaks (Morris, pers. comm.).

Other factors such as corrosion due to elements such as the pH of the water, moisture content, resistivity of the pipe material, and redox potential (metal electrical potential) may cause

damage that leads to localized leaks. These events tend to cluster in areas of certain characteristics. The Prescott Road and Texas Street's aging infrastructure consists of a high percentage of cast iron material mains that are susceptible to corrosion. Further investigation is necessary to explore the possibility of corrosion effects to the Company's system.

CHAPTER 5
SUMMARY AND CONCLUSIONS

The Baton Rouge Water Company (BRWC) serves over two hundred and forty thousand customers. It is a complex network of approximately 8.1 million linear feet of water mains, 65 wells, 39 pump stations, 15 house pumps, 12 enclosed storage facilities, 1 booster station, and 1 reservoir. The Company's water system is comprised largely of cast iron (roughly 41%) and polyvinyl chloride (roughly 23%).

Transient surges occur in a rapid period of time shifting from one steady state to another. It is commonly termed as water hammer. The disrupted state of the pressure waves propagate through the distribution system. The degree of severity of transient event pressures, created by a particular change in velocity, is dependent on the geometry of the water system, the amount in velocity change, and the speed of the wave in a particular system. Vacuum pressures that develop within a pipe may cause vapor cavities which can have adverse effects on pipes such as pipe collapse.

Surge models are available that can predict the extent of transients and variations in pressure, under current or hypothetical conditions of a system. However, modeling an entire distribution system in a proper manner, accounting for the specific characteristics of components in a system, requires extensive research and time. Spatial analysis is an effective method to employ in large distribution systems, such as the Baton Rouge Water Company's system, in an effort to isolate areas of concern. Thence, the areas of concern can then be further investigated.

Spatial statistics allows for the comparison of the spatial distribution of features in a geographic area to an assumed random spatial distribution. Generally speaking, the basis of comparison is expressed by the dispersion of the values around the mean (standard deviation or variance). A statistical analysis performed in a dataset will show whether a trend or a pattern

exists and whether it is statistically significant, that is, if the distribution differs from a random distribution.

Three particular spatial analysis techniques were chosen to uncover possible clustering patterns in the Baton Rouge Water Company's system: nearest neighbor, multi-distance spatial cluster analysis (Ripley's K function), and hot spot analysis (G_i* statistic).

The nearest neighbor analysis is a quick and effective means to discover if a set of data points exhibit a pattern that is clustered, dispersed, or simply random in nature. The solution is a Z-score value denoted either as a negative number smaller than -1.96 for clustering events, or a positive Z-value score greater than 1.96 for dispersed events at the 95% confidence level. The larger the negative number the greater the clustering of events and vise-versa. The result of the analysis for the study area, -66.39 (section 4.1), signifies a clustered pattern.

The multi-distance spatial cluster analysis (Ripley's K-function) is a descriptor of the extent to which spatial dependence exists in the distribution of the events. The K-function is useful in determining the distance, or distances, that exhibit clustering. Values that are statistically significant fall outside of the confidence envelope. A positive difference between the expected and the observed values indicate clustering and are statistically significant if the observed values fall outside the confidence envelope. The highest positive difference between the observed and the expected is the point where clustering is most pronounced. The peak for this study, at a 99% confidence level, is at 6,389 feet or 1.21 miles. A short enough distance for leak events that may be related to power failure, or pump trip, induced transients. This is the distance used in the hot-spot analysis.

The hot spot analysis (G_i* statistic) identifies clusters of features with similar values of a particular characteristic. A high Z-score for a feature indicates neighbors with high attribute

values and a feature with low Z-score value indicates neighbors with low attribute values at a given distance. A statistically significant Z-score is either lower or higher than the confidence limits, that is, falls outside the standard normal distribution; for a 95% confidence level, a Z-score that is either greater than 1.96 (clustering of high values) or less than -1.96 (clustering of low values). The result of this analysis is shown on figures 7 and 8 where clustering of high incident leaks surround the Prescott Road and the Texas Street tank stations.

The Prescott Road and Texas tank stations contain infrastructure that is over fifty percent cast iron and over fifty years of age (Table 6) leading to a greater susceptibility to breaks stemming from transient, shrink and swell, or corrosive environments (Figure 19). Both of these stations are also comprised of over twenty percent PVC piping that is vulnerable (Figure 19) to pipe collapse under vacuum pressures during a transient event.

A frequency analysis of power failure events for the study area (Table 7) reveals that Prescott Road and Texas Street do not have the highest pump failure rate. The amount of failures still warrants closer investigation. The pump failure and leak events were plotted (Figures 9 and 10). However, no evident correlation can be made since the times of power failure occurrences are not followed by a noticeable increase in leak events in the days and few weeks that follow. The leak events time of occurrence form concentrations much later in time. Leak events must appear within days or a few weeks of a power failure to merit theorizing a temporal relationship.

A comparison of the resulting leak clusters near pump stations were made with hydraulic surge models of the same areas. The results of the modeling reveal that the lowermost pressure that is reached following a pump trip simulation is 48.7 psig for the Prescott Road site (Figure 17) and 42.6 psig for the Texas Street site (Figure 18) for the Texas tank site.

Sub-atmospheric pressures of -14 psig and below must be achieved for cavitation to occur and for possible pressure spikes, which may follow, to arise.

Shrink and swell damage was quickly dismissed by simply mapping the mains vulnerable to expansive soils against spatial soil data classified by each soil's shrink-swell potential.

Undoubtedly, the concentration of leaks near the Prescott Road and Texas Street sites cannot be correlated with pump failure transients. Nevertheless, other types of surge, such as valve operation and fluctuating pressures, may possibly be responsible for causing damage that leads to leaks. Moreover, the aging infrastructure in the Prescott and Texas tank areas may facilitate damage from pressure surges and corrosion. Further investigation of both surge and corrosive environments is suggested.

Additionally, capturing information in the Quality Assurance report such as the condition of the impaired pipe and cause of the pipe failure is recommended. This would greatly diminish the time and level of research necessary to resolve issues relating to leak concerns.

REFERENCES

AWWA, 2004 (4th ed.). Manual M11, Steel Water Pipe – A Guide for Design and Installation. (AWWA: Denver).

AWWA, 2002. Manual M23, PVC [polyvinyl chloride] Pipe – Design and Installation. (AWWA: Denver).

AWWA, 2000. C403-00, Selection of Asbestos – Cement Transmission Pipe, Sizes 18in. Through 42 in. (AWWA: Denver).

Beecher, J A. and Flowers, J. E., 1999. Conservation Matters - Keep Track of That Water! Water Accounting for Management and Conservation. OPF, Vol. 25 Issue 5, p.p. 6-7, 10-11.

Bailey, T.C. and Gatrell, A.C., 1995. Interactive Spatial Data Analysis (Harlow: Longman Scientific and Technical).

Committee Report -- Water Accountability; AWWA Leak Detection and Water Accountability Committee, 1996. Journal American Water Works Association, Vol. 88, Issue 7, p.p. 108-111.

Dixon, P.M., 2002. Ripley's K Function. Encyclopedia of Environmetrics, Vol. 3, pp. 1796-1803.

Ductile Iron Pipe Research Association (DIPRA), 2004 (2006 Revision). The Design Decision Model for Corrosion Control of Ductile Iron Pipelines. (DIPRA: Birmingham).

Gatrell, A.C., Bailey, T.C., Diggle, P.J. and Rowlingson, B.S., 1996. Spatial Point Pattern Analysis and its Application in Geographical Epidemiology. Transactions of the Institute of British Geographers, New Series, Vol. 21, No. 1, pp. 256-274.

Getis, A., 2008. A History of the Concept of Spatial Autocorrelation: A Geographer's Perspective. Geographical Analysis, Vol. 40, No. 3, pp. 297-309.

Getis, A. and Aldstadt, J., May 2004. Constructing the Spatial Weights Matrix Using a Local Statistic. Geographical Analysis, Vol. 36, No. 2, pp. 90-104.

HDR Engineering, Inc., 2001. Handbook of Public Water Systems, 2nd Edition (New York: John Wiley & Sons, Inc.).

Hollis, P.R. (President, Owen & White Inc. Consulting Engineers; Professional Engineer). Personal communication. October, 2009 – March 1, 2010.

Holtz, R.D. and Kovacs, W.D., 1981. An Introduction to Geotechnical Engineering (Englewood Cliffs: Prentice-Hall, Inc.)..

Jung, B.S., Karney, B.W., Boulos, P.F. and Wood, D.J., 2007. The Need for Comprehensive Transient Analysis of Distribution Systems. Journal American Water Works Association, Vol. 99, Issue 1, pp. 112-123.

Lingireddy, S., Wood, D.J. and Zloczower N., 2007. Pressure surges in pipeline systems resulting from air releases. Journal American Water Works Association, Vol. 96, Issue 7, p.p. 88-94.

Mitchell, A., 2009. The ESRI Guide to GIS Analysis – Volume 2: Spatial Measurements and Statistics (Redlands: ESRI Press).

Morris, C. (Hydraulic Systems Analyst, Owen & White, Inc., Consulting Engineers). Personal communication. October, 2009 – October, 2011.

Morris, C., 2011. Surge Model Simulations of the Prescott Street and Texas Road Tanks for the Baton Rouge Water Company conducted at Owen & White Consulting Engineers in October of 2011.

Moser, A.P. and Folkman, S., 2008. Buried Pipe Design, 3rd Edition (New York: McGraw-Hill).

Natural Resources Conservation Service, 2010. East Baton Rouge Parish, Louisiana, Soil Survey. Survey Area Ver. 7 (02/08/2010).

Owen, E. (Chairman, Utilities Holdings; Professional Engineer). Personal communication. August, 2010 – December, 2010.

Phalempin, G., 2009. Highway 964 – Surge 2010 Analysis. Charlatte America, Fayat Group, Hydraulic Vessel Division Report. Revision 1, p.p. 1-9.

Ray Clayton, 1973. Baton Rouge Water Works Company. The Pipeline, Vol.1, No. 11.
The Baton Rouge Water Company, 2009. SCADA Monthly Water Production Report.

The Baton Rouge Water Company, 2006-2010. Quality Assurance Log, October 15, 2006 – January 19, 2010.

The Baton Rouge Water Company, 2006-2010. SCADA AlarnView Log, October 15, 2006 – January 19, 2010.

The Baton Rouge Water Company, 2009. Unaccounted For Water Summary.

The Baton Rouge Water Company, 2008. Unaccounted For Water Summary.

Thornton, J., Sturm R. and Kunkel G., 2008. Water Loss Control, 2nd edition (New York: McGraw-Hill).

Walski, T.M., Chase, D.V., Savic, D.A., 2001. Water Distribution Modeling, 1st Edition (Waterbury: Haestad Press).

Water Resources Update, 1991. Water Resources Infrastructure. Universities Council on Water Resources, Issue No. 86, p.p. 20-22.

Wood, D. J., Lingireddy, S., Boulos P.F., Karney, B.W., McPherson, D.L., 2005. Numerical Methods for Modeling Transient Flow in Distribution Systems. Journal American Water Works Association, Vol. 97, Issue 7, p.p. 104115.

Wood, D. J., 2005. Waterhammer Analysis – Essential and Easy (and Efficient). Journal of Environmental Engineering, Vol. 131, No. 8, pp. 1123-1131.

Wood, D.J. (Professor Emeritus, University of Kentucky; Director, KYPIPE L.L.C.). Personal communication. April and October, 2011.

Wood, D.J., Lingireddy, S. and Boulos P.F., 2005. Pressure Wave Analysis of Transient Flow in Pipe Distribution Systems (Pasadena: MWH Soft).

Woodall, C., 2002. Point pattern analysis of FIA data. Proceedings of the Third Annual Forest Inventory and Analysis Symposium; Gen. Tech. Rep. NC-230. St. Paul, MN: U.S. Department of Agriculture, Forest Service, North Central Research Station: 162-170.

APPENDIX
A LETTER OF PERMISSION

From: don wood [mailto:donjwood@gmail.com]
Sent: Sunday, October 23, 2011 6:01 PM
To: Dina Knight
Subject: Re: Thesis presentation

Dina:

You are welcome to use these slides. Good luck!

Don

--
Dr. Don J. Wood
Professor Emeritus, University of KY.
Director, KYPIPE LLC
www.kypipe.com

From: Dina Knight
Sent: Sunday, October 23, 2011 3:00 PM
To: 'don@kypipe.com'
Subject: RE: Thesis presentation

Dr. Wood,

In April of this year I asked for permission to use some of your graphics in my thesis presentation. I would like to ask for permission to use two graphics in my thesis document as well. These are the "Events following a pump trip" (slide 29) and the "Pressure Wave Speed" (graphic only on slide 48). Please let me know if that is acceptable.

Thank you kindly,
Dina S. Knight
Senior GIS Analyst
The Baton Rouge Water Works Company

From: don wood [mailto:donjwood@gmail.com]
Sent: Monday, April 04, 2011 4:28 PM
To: Dina Knight
Subject: Re: Thesis presentation

Dina:

You are certainly welcome to use any of the slides I presented in your presentation. If I can be of any help please let me know. Certainly transients in the BR water system would be of interest to me - especially looking at large distribution system models. Good Luck!

Don

--
Dr. Don J. Wood
Professor Emeritus, University of KY.
Director, KYPIPE LLC
www.kypipe.com

From: Dina Knight
Sent: Monday, April 04, 2011 11:51 AM
To: 'don@kypipe.com'
Subject: Thesis presentation

Dr. Wood,

My name is Dina and I am currently working on my Masters at LSU. My topic relates to your expertise, transient events. I watched your webcast (Surge Analysis Modeling – an Essential and Manageable Task for Engineers) with IDModeling, which I thoroughly enjoyed. I would like to request your permission to use some of the graphics shown on the webcast in my thesis presentation in the fall. Please let me know if that is acceptable.

Thank you kindly,

Dina S. Knight
Senior GIS Analyst
The Baton Rouge Water Works Company

VITA

Dina Knight is married and a native of Brazil. She has resided in the United States for the past thirty one years. Ms. Knight has dual citizenship in the United States and in Brazil and speaks Portuguese fluently. Her life in the United States began in the state of New Jersey. Ms. Knight earned her Bachelor of Arts degree in Geography from Rutgers, The State University of New Jersey. She began her geospatial career at the Delaware Department of Transportation followed by the New Castle Conservation District before accepting the position as a Research Associate at Louisiana State University. Ms. Knight was a Research Associate at Louisiana State University from January of 2000 until October of 2007. The majority of those years were spent at the Center for GeoInformatics where she gained valuable knowledge in the area of Global Positioning Systems, Real Time Networks, Virtual Reference Stations, along with furthering her geospatial aptitude. She continues her career at the Baton Rouge Water Works Company and is currently holding the position of Senior GIS Analyst.